University of Central Florida
STARS

Honors Undergraduate Theses | UCF Theses and Dissertations

2022

COVID-19 and Diabetes

Radhika Desai
University of Central Florida

 Part of the Endocrinology, Diabetes, and Metabolism Commons
Find similar works at: https://stars.library.ucf.edu/honorstheses
University of Central Florida Libraries http://library.ucf.edu

This Open Access is brought to you for free and open access by the UCF Theses and Dissertations at STARS. It has been accepted for inclusion in Honors Undergraduate Theses by an authorized administrator of STARS. For more information, please contact STARS@ucf.edu.

Recommended Citation

Desai, Radhika, "COVID-19 and Diabetes" (2022). *Honors Undergraduate Theses*. 1259.
https://stars.library.ucf.edu/honorstheses/1259

COVID-19 AND DIABETES

by

RADHIKA DESAI

A thesis submitted in partial fulfillment of the requirements
for the Honors in the Major Program in Biomedical Sciences
in the College of Medicine
and in the Burnett Honors College
at the University of Central Florida
Orlando, Florida

Spring Term, 2022

Thesis Chair: Robert Borgon, Ph.D.

Abstract

Patients with Type 2 Diabetes (T2D) have been found to have increased mortality and morbidity for COVID-19 and are at higher risk for severe disease once infected with COVID-19. Clearly, there exists a relationship between T2D and COVID-19 that requires more attention. In order to understand the mechanisms by which T2D contributes to more severe COVID-19 disease, attention was turned to extracellular vesicles (EVs). It was speculated that viral RNA components of the COVID-19 virus may have originated from circulating EVs that came from infected cells and use a Trojan Exosome method to infect host cells. It is necessary to characterize the EVs and viral RNA components of COVID-19 patients to understand the infection mechanisms. EV purification, liquid chromatography-tandem mass spectrophotometry, nanoparticle tracking analysis, Real Time-Polymerase Chain Reaction (qPCR), and Bioanalyzer analysis were performed for this using patient samples from Advent Health Orlando. Results found that qPCR was unable to detect COVID-19 viral RNA in the EVs of these patients, most likely a result of poor sensitivity. This study contributes towards defining the proteomic landscape of circulating EVs in people with COVID-19 and T2D and identifying biological mechanisms driving the interaction between the two diseases. Future directions include profiling the small noncoding RNAs found in COVID-19 patients and utilizing different methods to analyze isolated RNA to identify COVID-19 viral materials in EVs.

Table of Contents

List of Tables

List of Figures

Introduction

In December 2019, an outbreak of the severe acute respiratory syndrome caused by a highly infectious RNA virus led to a severe acute respiratory syndrome coronavirus 2 (SARS-CoV-2) pandemic. This has been coined the Coronavirus disease 2019, or COVID-19 pandemic. The structure of the virus is as such: positive-sense single-stranded RNA genome and a nucleocapsid of helical symmetry. The virus also contains a protein envelop with "crown-like" spike projections that allow the virus to bind to angiotensin-converting enzyme (ACE2), found on the membrane of pulmonary cells, among main tissues (Rajpal, Rahimi, Ismail-Beigi, 2020). This enzyme is the key component that mediates the internalization of the virus. The COVID-19 virus primarily infects the upper respiratory and gastrointestinal tracts and can cause pneumonia in the lower respiratory tract (Erener, 2020).

The virus pathology has three stages (Erener, 2020). Stage I is the early infection phase and is met with symptoms such as a fever, dry cough, and headache. Stage II is the pulmonary phase and results in shortness of breath and abnormal chest images. Lastly, stage III is the hyperinflammation phase. Here, the virus stimulates the immune system, resulting in a strong inflammatory and hyperimmune response, called a "cytokine storm." It is so deemed because of the elevated inflammatory markers that result in acute respiratory distress syndrome, shock, multiorgan failure, and sometimes death. Characteristic of the viral infection are a variety of side effects including massive bilateral viral pneumonia, acute respiratory distress syndrome, cardiac and kidney injury, hypercoagulation and stroke, liver damage, infection of pancreatic islets, and multiple organ failure (Rajpal, Rahimi, Ismail-Beigi, 2020).

In the past two years, patient data has found that a high percentage of severely ill COVID-19 patients often have one or more comorbidities, including increased age, hypertension, type 2 diabetes (T2DM), obesity, dyslipidemia, renal and cardiovascular disease. With that, an increase in mortality and morbidity with COVID-19 has been found to be associated with diabetes, deeming the chronic disease one of the leading comorbidities associated with COVID-19 infection severity (Erener, 2020). The incidence of patients in intensive care for COVID-19 having diabetes is twofold higher when compared to the incidence of patients in intensive care for COVID-19 without diabetes (Erener, 2020). Further, the mortality of COVID-19 has been found to be approximately threefold higher in those patients with diabetes than those without (Erener, 2020). A whole-population study conducted in England found an increased risk of in-hospital death by COVID-19 in people with diabetes. Even after adjusting for age, sex, ethnicity, socioeconomic deprivation, and region, individuals with diabetes had a greater risk of in-hospital death caused by COVID-19 than those without diabetes (Barron, 2020). Thus, it is clear that there is a relationship between diabetes and COVID-19 that requires more medical intervention and attention.

Diabetes is a chronic disease that is characterized by high blood glucose levels and an impairment in insulin action and/or secretion. The incidence of diabetes worldwide is immense: over 425 million individuals have diabetes worldwide– as of 2020– and this number is projected to rise to 629 million by 2045 (Erener, 2020). There are two forms of diabetes: type 1 (T1D) and type 2 (T2DM). In T1D, insulin-producing beta cells are destroyed by the autoimmune system. In T2DM, there is a combination of insulin resistance and a secretory defect in the beta cells' insulin system that drive the beta cells into exhaustion and eventually destruction (Erener, 2020).

Individuals with diabetes have been found to have an altered immune system where they are more at risk for infections and complications. Research has found that hyperglycemia results in a decrease in intestinal barrier function– making individuals more susceptible to bacterial entry– and dysregulations in immune function (Erener, 2020). These studies have also found that patients with T2DM may have changes in their innate immune system that promote the production of pro-inflammatory cytokines and have a defective host defense system against viral infections (Rajpal, Rahimi, Ismail-Beigi, 2020). These changes increase the risk for infections and result in a greater number of hospitalizations and higher mortality (Erener, 2020).

Although there exists an association between COVID-19 and both forms of diabetes, our research was focused on T2DM specifically (Powers, Aronoff, and Eckel, 2021). T2DM patients are often more vulnerable to contract infections, however it is not clear whether that is the case with COVID-19. It is clear, though, that patients with T2DM are at higher risk for severe disease once they are infected with COVID-19. There are a variety of factors that can explain the higher morbidity and mortality of patients with T2DM and COVID-19, including ACE2 expression, hyperglycemia, and increased coagulopathy to name a few (Rajpal, Rahimi, Ismail-Beigi, 2020). These factors are associated with an increased susceptibility of patients with T2DM to COVID-19 infection (Rajpal, Rahimi, Ismail-Beigi, 2020).

ACE2 expression is one potential factor that can result in a more severe COVID-19 infection for diabetic patients. Angiotensin-2 is an eight amino acid peptide. The enzyme angiotensin-converting enzyme 1 (ACE1) catalyzes the conversion of angiotensin-1 to angiotensin-2. Then, angiotensin-2 works to stimulate aldosterone secretion, increase sodium retention and blood pressure, increases vascular permeability in lungs, and elicits an

inflammatory response. Angiotensin converting enzyme 2 (ACE2) is a plasma membrane protein that is expressed largely in the lungs, tissues, endothelial cells, and insulin producing beta cells. COVID-19 has a high affinity toward ACE2 where, when the virus binds, the associated complex is internalized. Following intracellular replication of the virus, ACE2 will act as a receptor for the virus. This is the dominant path of entry for the virus into the lung. In diabetic patients, ACE2 expression is increased in response to elevated glucose levels. Thus, diabetic patients have a higher susceptibility to contract the disease (Rajpal, Rahimi, Ismail-Beigi, 2020).

Hyperglycemia's role in the relationship between diabetes and COVID-19 has been studied as well. Translating directly to "high blood sugar," hyperglycemia describes a state of high blood glucose that can be a result of reduced insulin secretion, decreased glucose utilization, and increased glucose production (Mouri and Badireddy, 2021). Hyperglycemia has been found to increase the expression of ACE2 "receptor" sites in the pulmonary system of patients with diabetes (Rajpal, Rahimi, Ismail-Beigi, 2020). This allows for greater opportunity for viral infection. Thus, patients with diabetes and hyperglycemia are more prone to developing severe disease. The high glucose levels of hyperglycemia also cause collagen to be less susceptible to proteolysis which leads to accumulation of connective tissue in the lungs and restrictive lung disease, and the promotion of proinflammatory cytokines that lead to oxidative stress (Rajpal, Rahimi, Ismail-Beigi, 2020). Research has found that patients admitted with COVID-19 with either diabetes or uncontrolled hyperglycemia had higher mortality and longer hospitalizations (Rajpal, Rahimi, Ismail-Beigi, 2020). Cohort analyses and retrospective studies of COVID-19 patients in China and the United Kingdom have found that hyperglycemia and poor glycemic control are predictors of worst chest radiographic imaging results and associated with high risk

of in-hospital death (Apicella, et al., 2020). In fact, hyperglycemia, even in people without diabetes, worsens the prognosis and increases the mortality risk of COVID-19 (Ceriello A. Diabetes Res Clin Pract. 2020; Ceriello, De Nigris, and Prattichizzo, Diabetes Obes Metab. 2020). Thus, glycemic control has been found to be associated with improved outcomes in COVID-19 and T2DM patients and poor glycemic control and hyperglycemia are associated with negative outcomes for COVID-19 patients (Ayres, 2020).

Coagulopathy also explains the worse disease progression of COVID-19 in diabetic patients. COVID-19 has been found to be associated with increased coagulation activity. During infection, intra-vessel coagulation, changes in lung vessels, endothelial injury, and the growth of new vessels have been identified as changes as a result of endothelial dysfunction (Apicella, et al., 2020). Diabetes is associated with a prothrombic state due to the imbalance between clotting factors and fibrinolysis and the increased risk of thromboembolic events (Apicella, et al., 2020). Thus, COVID-19 patients with diabetes are at risk for hypercoagulation and thrombotic complications that worsen their disease states.

The interactions between COVID-19 and diabetes demonstrate a need to understand the mechanisms by which T2DM contributes to more severe COVID-19 disease. Thus, a way by which these mechanisms can be studied is necessary. In general, attention has recently turned to extracellular vesicles (EV) to understand disease mechanisms because of their increased stability, abundance in biofluids, and because their content (cargo) mirror to some extent that of the originating cells. EVs is a general term used to refer to all the vesicles secreted by cells, which include smaller size exosomes (~30-140 nm) that are derived from multivesicular endosome-based secretions and microvesicles (~100-1000 nm) derived from the plasma membrane

(Hessvik and Llorente, 2018). They are found in nearly all biological fluids and are representative of their parent cells. Further, they carry a variety of molecules, including proteins, miRNAs, and lipids, that are involved in the physiological and pathological processes of various diseases (Nunez Lopez, et al., 2021). Analyzing the EV protein cargo may provide insight on the mechanisms by which T2DM contributes to more severe COVID-19 disease. It is hypothesized that EVs may contribute to COVID-19 disease progression in diabetic patients and that EVs secreted by virus-infected cells contain cell-derived and virus-derived components; thus these hypotheses can be studied by analyzing EV cargo.

Further, the analysis of EV cargo has been found to be of good potential for novel biomarker development and future disease diagnosis. Biomarkers are clinically significant for their use in improving diagnostic capacity, predicting progression and risk of chronic complications, and evaluating treatment efficacy (Barile and Vassalli, 2017). An ideal biomarker is defined as "one through which the disease comes about or through which an intervention alters the disease" (Aronson, 2005). Due to the fact that all cells and all individuals, regardless of disease status, secrete EVs with different contents into both circulation and bodily fluids, the use of EVs as biomarkers for disease has been studied (Barile and Vassalli, 2017). These EV-based disease biomarkers can be identified before symptoms occur, deeming them as beneficial candidates for disease detection. Both healthy subjects and patients with different diseases will release EVs that have different contents and these cargoes can be measured for diagnostic purposes (Barile and Vassalli, 2017). Studying EV protein cargo in the context of diabetes and COVID-19 will help identifying biomarkers of increased risk for COVID-19 in diabetic patients and identifying new targets for therapies to improve outcomes and decrease resulting morbidity and mortality.

To study the EV protein cargo in our study, proteomics will be utilized. Proteomics is the study of the proteome, the full set of proteins expressed by an organism in a specific cell or tissue at a certain time (Cañadas-Garre M, et al, 2019). Proteomic studies can be done using a multitude of different lab techniques, including gel electrophoresis and mass spectrometry.

Although it is not fully understood whether EVs contribute to SARS-CoV-2 infection and COVID-19 progression, the role of EVs has been studied to gain an understanding of the disease's mechanisms. An interesting finding is that enveloped RNA viruses, such as SARS-CoV-2, share similar characteristics with EVs, including size and physicochemical properties (Margolis and Sadovsky, 2019). Due to this, some of these viruses are able to hijack the endocytic pathway that is normally used for EV biogenesis in order to assemble and secrete viral particles (Nunez Lopez, Casu, and Pratley, 2021). Due to this, EVs are potentially hypothesized to be "close relatives" of enveloped viruses, suggesting either an evolutionary relationship or supporting the "Trojan exosome" hypothesis. The "Trojan exosome" hypothesis explains the role of extracellular vesicles in transporting viral particles and genomes to susceptible host cells (Altan-Bonnet, 2016). It states that some viruses will use the preexisting, nonviral exosome biogenesis pathway to form infectious particles and escape immune surveillance (Gould, Booth, and Hildreth, 2003).

For example, studies have found that the full virion of the non-enveloped hepatitis A virus (HAV) can hide inside the host-derived exosome-like vesicles and then become protected from antibody-mediated neutralization; this allows for the virus to infect and replicate in the liver in a stealth manner (Feng, et al., 2013). This method provides many benefits to virus, including

being able to deliver the virions to target cells at higher concentrations, “enabling multiplicities of infection” (Santiana, et al., 2018).

It has been found that EVs secreted by virally infected cells may contain both cell-derived and virus-derived components (Nunez Lopez, Casu, and Pratley, 2021). Viral microRNA (miRNAs), proteins, or entire virions can be incorporated into EVs and then promote or restrict the replication of the virus in target cells (Nunez Lopez, Casu, and Pratley, 2021). Exosomal RNAs are protected from degradation by being placed inside the vesicles (Badierah, Uversky, and Redwan, 2020). In order to detect this RNA content, quantitative PCR (qPCR) is conducted. Doing so can shed light on whether viruses can manipulate the biogenesis of exosomes to enhance their own transmission and infection by transferring viral particles and RNA to other cells (Badierah, Uversky, and Redwan, 2020).

In the context of SARS-CoV-2, it is speculated that viral RNA components of the virus may have originated from circulating EVs that came from infected cells (Elrashdy, 2020). Thus, it is necessary to characterize the EVs and viral RNA components of SARS-CoV-2 patients to understand the infection mechanisms. Our research is significant because, currently, there is little evidence on the role of EVs on the pathogenesis of SARS-CoV-2 infection (Nunez Lopez, Casu, and Pratley, 2021). Thus, confirmation of the existence of SARS-CoV-2-laden trojan vesicles in the extracellular space and/or patient’s circulation is necessary. This method, if confirmed, could then be manipulated to stop the spread of and treatment of SARS-CoV-2 virus.

Hypothesis

Our overarching hypothesis is that diabetes-related changes in the plasma proteome are associated with the increased severity of COVID-19 in patients with both SARS-CoV-2 infection and diabetes and these relationships could be identified by profiling circulating extracellular vesicles. More specifically, we hypothesize that diabetes contributes to a state of enhanced hypercoagulability and hyper-inflammation during SARS-CoV-2 infection via diabetes-specific EV signals. We further hypothesize that circulating EVs from SARS-CoV-2 infected subjects may contain viral RNA cargo.

To assess our hypothesis, our study will define the EV proteomic landscape in people with COVID-19 with or without diabetes, compared to people with alternative (non-SARS-CoV-2) acute respiratory infection in equivalent diabetic background and address the following aims by implementing linear models with an interaction term.

Aims

Aim 1: To isolate circulating EVs from archived plasma samples from hospitalized patients with COVID-19 and assess whether the disease affects the concentration of circulating EVs and whether the EVs carry SARS-CoV-2 RNA. This aim will allow us to characterize the profile of circulating EVs in patients with COVID-19, in the presence or not of concomitant T2DM. A strength of our analysis is that we will compare these profiles to proper control groups comprised of patients with an alternative diagnosis of (non-SARS-CoV-2) acute respiratory disease (RSP), with and without T2DM.

Aim 2: To define the proteomic landscape of the EVs circulating in the plasma of patients with either COVID-19 or alternative RSP, with or without T2DM, who needed hospitalization. This aim will allow us to gain mechanistic insight and identify potential biomarkers associated with the characteristic interaction between COVID-19 and T2D.

Study Cohorts

This cross-sectional study was conducted in accordance with applicable Federal regulations and institutional research policies and procedures. The study included 4 groups with 12 participants each:

- Cohort 1. COVID-19 with T2DM
- Cohort 2. COVID-19 without T2DM
- Cohort 3. RSP with T2DM
- Cohort 4. RSP without T2DM

Study participants were identified from patients hospitalized at AdventHealth with a Covid-19 (SARS-CoV-2 PCR positive) or alternative (SARS-CoV-2 PCR negative) acute respiratory infection (RSP) diagnosis from the range of June to August of 2020. Important effects were made to ensure the homogeneity of the study cohort. From the pool of 1,061 patients, 494 were hospitalized; 431 were hospitalized but never went to the intensive care unit (ICU), 45 were hospitalized and later went to the ICU, and 18 were hospitalized and were directly admitted to the ICU. Patients younger than 20 years of age, with T1D, that were pregnant, or went directly to the ICU were excluded. From the original 1,061 patients, 106 patients total fit these criteria. This cohort was subset for race/ethnicity, including only the study included black African American (AA), white Hispanic/Latino (H/L), and non-Hispanic white (NHW) people as other races and ethnicities were not well represented.

This cohort included 87 participants, from which random cohort selection was conducted to produce the final optimal cohort. To guarantee generalizability of our results, equal number of males and females from each race/ethnicity was included as a constraint, whenever possible. A

total of 10,000 random cohorts were generated and differences among variables were assessed using the Fisher test for categorical variables and ANOVA for continuous variables. Random cohorts were then ranked by the averaged P value for 3 key comparisons including age, lag-time (time samples remained stored at 4ºC before long-term storage at -80ºC in the biorepository) and time difference between sample collection and hospitalization (constrained to a maximum of five days). The optimal random cohort did not include patients with ICU events, because only two were include in the final set used for random cohort selection.

Methods

EV Purification: Plasma EVs were isolated by Tymora Analytical Operations (Tymora, Lafayette, IN) using Extracellular Vesicles total recovery and purification' (EVtrap) technology, a novel magnetic bead approach that utilizes chemical affinity for EV capture and purification.

Liquid chromatography-tandem mass spectrophotometry (LC-MS/MS): LC-MS/MS proteomics was conducted by Tymora as described by Nunez Lopez and colleagues (2021).

Nanoparticle Tracking Analysis (NTA): NTA was performed with a NanoSight NS300 and the NTA-3.4 software (Malvern Panalytical, MA). Detection of nanoparticles in a diluted EV sample is achieved using dynamic light-scattering technology. Our instrument was equipped with a 488 nm blue laser module, flow-cell top plate, integrated temperature control, and a single-syringe pump module. Samples were diluted using cell culture grade water (Corning cat# 25-005-CI) to produce an optimal particle concentration for final measurement in the range of 10^7 to 10^9 particles/ml. Final quantification included 5 standard measurements of 1 minute of duration each, taken at a controlled temperature of 25°C and under constant recommended automatic flow. Camera level for video capture was set to 12 and detection threshold to 5 for all sample measurements.

RNA characterization: Real Time-Polymerase Chain Reaction (qPCR) was used to detect Covid-19 viral RNA. In short, total RNA from a small aliquot of EV preparation (from 50 µL of plasma) was purified using Qiagen miRNeasy micro kit (Qiagen, CA) following the

manufacturer's instructions. Yield and quality of the total RNA preparations were determined using the Agilent 2100 Bioanalyzer (Agilent, CA). Expression of 2 viral genes (N1 and N2) that are used to detect cases of COVID-19 and a human control gene (RNase-P) using the SARS-CoV-2 Research Use Only qPCR Primer & Probe Kit: N1, N2 & RP (2019-nCoV RUO Kit) from Integrated DNA Technologies was assessed by qPCR using a ViiA-7 instrument from ThermoFisher Scientific (Waltham, MA), following manufacturers' instructions.

Statistical and bioinformatic analyses: This was performed by researchers in the lab. The Shapiro-Wilk test, the Welch two-sample t test (for continuous variables), and the Fisher exact test (for categorical variables) were used. Enrichment for KEGG pathways and gene ontology biological processes among the lists of differentially abundant EV proteins were assessed using the clusterProfiler R package. Enrichment for tissue-specific proteins among the differentially abundant EV proteins was assessed using custom R scripts developed at AdventHealth Translational Research Institute.

Results

Participants and study design

Important efforts were made to ensure the homogeneity of the study cohort. Participants were identified from patients hospitalized at AdventHealth with a COVID-19 (SARS-CoV-2 PCR positive) or alternative (SARS-CoV-2 PCR negative) acute respiratory infection (RSP) diagnosis during June-August 2020 and for which plasma samples were available in our biorepository. In summary, participants were required to be older than 20 years of age (three excluded). Out of the initial pool of 1061 patients, there were 494 that were hospitalized: 431 (87.25%) were patients that were hospitalized but never went to the intensive care unit (ICU), 45 (9.11%) were patients that were hospitalized and later went to the ICU, and 18 (3.64%) were hospitalized and went directly to the ICU. Only patients that were hospitalized but did not go directly to ICU were included. Participants were selected only if the biorepository samples were collected no more than five days before or after hospitalization and before the patient went to the ICU. A total of 106 patients fitted the above criteria. Two of these patients were reported to be pregnant and excluded from further analysis. The hospitalized cohort passing the above inclusion criteria was then subset for race/ethnicity to only include black African American (AA), white Hispanic/Latino (H/L), and non-Hispanic white (NHW) people. A total of 87 patients fit these criteria and were selected for random cohort selection, constrained by including equal number of males and females from each race/ethnicity, whenever possible. 10,000 random cohorts were generated and differences among variables assessed using the Fisher test for categorical variables and ANOVA for continuous variables. Random cohorts were ranked by the averaged P value for three key comparisons including age, lagtime (time samples remained stored at 4 C before long-term storage at -80 C in

the biorepository) and time difference between sample collection and hospitalization. The optimal random cohort did not include patients with ICU events because only two were included in the final set used for random cohort selection.

The clinical characteristics of the optimal complete study cohort are summarized in Table 1. This study design allowed us to effectively model and quantify the independent COVID-19 and T2D effects as well as the interaction between the two diseases, while adjusting for the potential confounding effect of age, gender, race, and ethnicity.

Table 1: Clinical Characteristics of Study Participants

	Group 1 (n=12)	Group 2 (n=12)	Group 3 (n=12)	Group 4 (n=12)	p
COVID.Dx = Positive (%)	12 (100.0)	12 (100.0)	0 (0.0)	0 (0.0)	<0.001
DM2.Dx = Positive (%)	12 (100.0)	0 (0.0)	12 (100.0)	0 (0.0)	<0.001
RSP.Dx = Positive (%)	0 (NA)	0 (NA)	12 (100.0)	12 (100.0)	NA
age (mean (SD))	69.75 (13.45)	67.17 (18.02)	71.50 (13.74)	68.00 (13.22)	0.892
patient_gender = Male (%)	6 (50.0)	6 (50.0)	6 (50.0)	6 (50.0)	1
patient_race = White (%)	6 (50.0)	8 (66.7)	8 (66.7)	10 (83.3)	0.392
ethnic_group = Non-Hispanic or Non-Latino (%)	10 (83.3)	10 (83.3)	10 (83.3)	11 (91.7)	0.919
race_ethnicity (%)					0.614
Black or African American_Non-Hispanic or Non-Latino	6 (50.0)	4 (33.3)	4 (33.3)	2 (16.7)	
White_Hispanic or Latino	2 (16.7)	2 (16.7)	2 (16.7)	1 (8.3)	
White_Non-Hispanic or Non-Latino	4 (33.3)	6 (50.0)	6 (50.0)	9 (75.0)	
Hospitalized. = YES (%)	12 (100.0)	12 (100.0)	12 (100.0)	12 (100.0)	NA
ICU.Patient. = NO (%)	12 (100.0)	12 (100.0)	12 (100.0)	12 (100.0)	NA
ICU.Event = NO (%)	12 (100.0)	12 (100.0)	12 (100.0)	12 (100.0)	NA
timediff_sample2hosp_h (mean (SD))	6.00 (20.78)	8.00 (18.68)	8.00 (21.30)	12.00 (19.15)	0.903
lagtime_h (mean (SD))	80.26 (17.83)	78.90 (15.77)	78.73 (27.19)	84.29 (11.88)	0.881
Glucose.Lvl (mean (SD))	174.60 (83.90)	111.50 (14.47)	151.64 (46.72)	105.78 (22.77)	0.019
CRP.Inflammatory (mean (SD))	130.10 (100.63)	96.84 (137.65)	NA (NA)	117.55 (103.45)	0.907
D.Dimer.Quant (mean (SD))	2.09 (1.36)	0.76 (0.40)	NA (NA)	3.33 (NA)	NA

Ferritin.Lvl (mean (SD))	852.40 (597.04)	951.00 (1208.95)	NA (NA)	98.00 (NA)	NA
INR (mean (SD))	1.61 (0.55)	1.12 (0.22)	1.31 (0.39)	1.15 (0.11)	0.481
Troponin.T (mean (SD))	0.01 (0.01)	0.00 (0.01)	0.72 (1.02)	0.00 (NA)	NA
Troponin.T.Interp (%)					0.497
GRAYZONE	1 (20.0)	0 (0.0)	0 (0.0)	0 (0.0)	
NEGATIVE	4 (80.0)	2 (100.0)	1 (50.0)	1 (100.0)	
POSITIVE	0 (0.0)	0 (0.0)	1 (50.0)	0 (0.0)	
CO2.Lvl (mean (SD))	23.30 (2.87)	24.50 (2.56)	24.09 (5.49)	23.33 (2.29)	0.876
ALT (mean (SD))	21.25 (12.98)	31.40 (11.17)	29.00 (19.94)	37.33 (26.16)	0.499
AST (mean (SD))	31.88 (18.54)	29.80 (6.53)	43.83 (22.16)	41.33 (30.17)	0.573
Albumin.Lvl (mean (SD))	3.18 (0.34)	3.46 (0.85)	3.13 (0.71)	3.57 (0.55)	0.653
Bilirubin.Total (mean (SD))	0.46 (0.35)	0.52 (0.22)	0.55 (0.44)	0.97 (1.00)	0.476
Creatinine.Lvl (mean (SD))	2.43 (3.03)	1.01 (0.27)	1.99 (2.08)	0.85 (0.38)	0.244
BUN.Lvl (mean (SD))	33.80 (27.37)	19.12 (17.36)	29.55 (22.40)	14.67 (10.06)	0.18
LD (mean (SD))	321.33 (90.96)	372.00 (41.39)	NA (NA)	297.50 (86.97)	0.549
Lactic.Acid.Lvl (mean (SD))	1.35 (0.33)	2.05 (0.64)	1.00 (0.28)	1.70 (0.71)	0.225
Calcium.Lvl (mean (SD))	8.86 (0.42)	8.76 (0.51)	8.95 (0.64)	8.59 (0.37)	0.449
Chloride.Lvl (mean (SD))	98.80 (6.56)	105.12 (8.56)	100.18 (4.79)	103.22 (6.40)	0.178
Potassium.Lvl (mean (SD))	4.35 (0.54)	4.12 (0.30)	4.35 (0.44)	3.93 (0.39)	0.123
Sodium.Lvl (mean (SD))	134.80 (5.14)	141.12 (9.01)	135.45 (4.46)	136.44 (5.94)	0.156
WBC (mean (SD))	8.32 (3.86)	7.12 (3.24)	9.53 (2.18)	8.90 (2.11)	0.456
Abs.Lymphocyte.Cnt (mean (SD))	0.93 (0.81)	0.95 (0.55)	1.87 (0.37)	1.72 (1.06)	0.078
Abs.Basophil.Cnt (mean (SD))	0.04 (0.09)	0.02 (0.02)	0.03 (0.01)	0.03 (0.02)	0.889
Abs.Eosinophil.Cnt (mean (SD))	0.02 (0.04)	0.06 (0.05)	0.37 (0.39)	0.20 (0.19)	0.03
Abs.Monocyte.Cnt (mean (SD))	0.55 (0.64)	0.40 (0.16)	0.69 (0.08)	0.73 (0.28)	0.575
Abs.Neutrophil.Cnt (mean (SD))	6.64 (2.99)	4.52 (2.80)	6.47 (1.69)	6.24 (1.98)	0.46
Lymphocytes (mean (SD))	13.61 (15.99)	18.52 (17.13)	20.50 (7.01)	19.80 (13.24)	0.82
Basophils (mean (SD))	0.48 (1.02)	0.30 (0.31)	0.38 (0.15)	0.30 (0.23)	0.955
Eosinophils (mean (SD))	0.34 (0.52)	0.95 (0.89)	3.82 (3.65)	2.40 (2.27)	0.033
Monocytes (mean (SD))	5.58 (3.20)	6.03 (1.85)	7.54 (1.87)	8.22 (3.40)	0.348
Neutrophils (mean (SD))	77.56 (18.11)	63.53 (23.55)	67.58 (9.11)	69.10 (17.44)	0.54

EV preparations are enriched in exosomal particles

Plasma EVs were isolated using Tymora's non-antibody-based affinity EVtrap proprietary technology (designed to quantitatively capture membrane-bound vesicles including exosomes).

EV proteins detected by LC-MS/MS were highly enriched in exosomal proteins (Figure 1A), including 87 of the top 100 Exocarta proteins (Figure 1B), reported to be the best exosomal markers. On the other hand, nanoparticle tracking analysis (NTA) using a NanoSight NS300 (Malvern Panalytical, MA) demonstrated size distributions consistent with preparations enriched in small extracellular vesicles (Figure 1C, D). Interestingly, increased particle concentration was demonstrated along most of the size range observed for the COVID-19 groups (Group 1 and Group 2), as compared to their respective non-COVID-19 controls (Group 3 and Group 4). However, the increase was not statistically significant (P>0.05) at the level of total particle concentration. Importantly, the multidimensional scaling plot of all EV proteomic data passing stringent filtering criteria suggested that circulating EV proteomics can effectively distinguish the 4 study groups (Figure 1E).

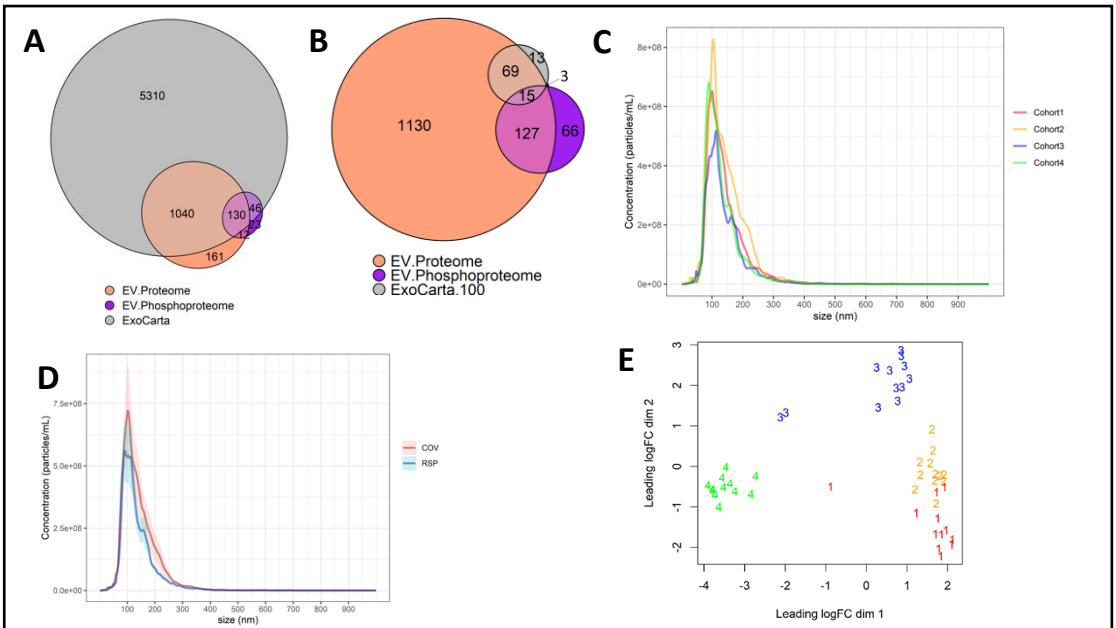

Figure 1. Characterization of plasma circulating extracellular vesicles (EVs) in hospitalized patients with either COVID-19 or alternative acute respiratory disease (RSP), with or without type 2 diabetes (T2D). (A,B) Venn diagrams of detected EV proteins cross-referenced to the complete Exocarta database (A) or the top 100 exosome markers in Exocarta (B). (C,D) Nanoparticle tracking analysis summarized by group (C) and by presence of COVID-19 (C) or alternative respiratory (RSP) (D) infection. (E) Multidimensional scaling (MSD) plot of Euclidean distances among cohorts based on the normalized abundance levels of all stringently detected EV proteins.

COVID-19 RNA was not detected in the EV preparations

RNA extracted from EVs isolated from a small aliquot of 50 µL of plasma and characterized using an Agilent 2100 Bioanalyzer demonstrated a larger amount of RNA in circulating EVs from the COVID-19 infected groups (Figure 2). While the region from 10-40nt displays the concentration of micro-RNA (miRNA), the region from 40nt onwards displays the concentration of other small noncoding RNAs, including tRNA fragments, Y-RNA, piRNA, full tRNA, and other types. The small RNA concentration in COVID-19 vesicles with T2DM was 1,506.7 pg/µl and in COVID-19 vesicles without T2DM was 3024.3 pg/µl. On the other hand, the small RNA concentration in RSP vesicles with T2DM was 874.8 pg/µl and in RSP vesicles without T2DM was 1542.8 pg/µl (Figure 2). Our findings demonstrate that COVID-19 vesicles (Figure 2A, 2B) have increased levels of noncoding small RNAs than RSP vesicles (Figure 2C, 2D) as is shown by the peak around 40 nt However, qPCR was unable to detect COVID-19 viral RNA in these preparations (Figure 3). Figure 3A and 3B display the amplification results of the viral N1 and N2 genes, respectively. While the control samples amplified, there was no sample amplification; this means that the N1 and N2 gene was detected in the sample but not our EV samples. Figure 3C displays the amplification results of a human control gene (RNase-P). Here, both the control and this internal control were both amplified. This demonstrates that our EV preparations contained quality RNA, however we could not detect viral RNA. We reason that our inability to detect SARS-CoV-2 RNA in the EV preparation may represent a sensitivity issue due to the expected low viral loads or contamination due to co-isolation of viruses with EVs.

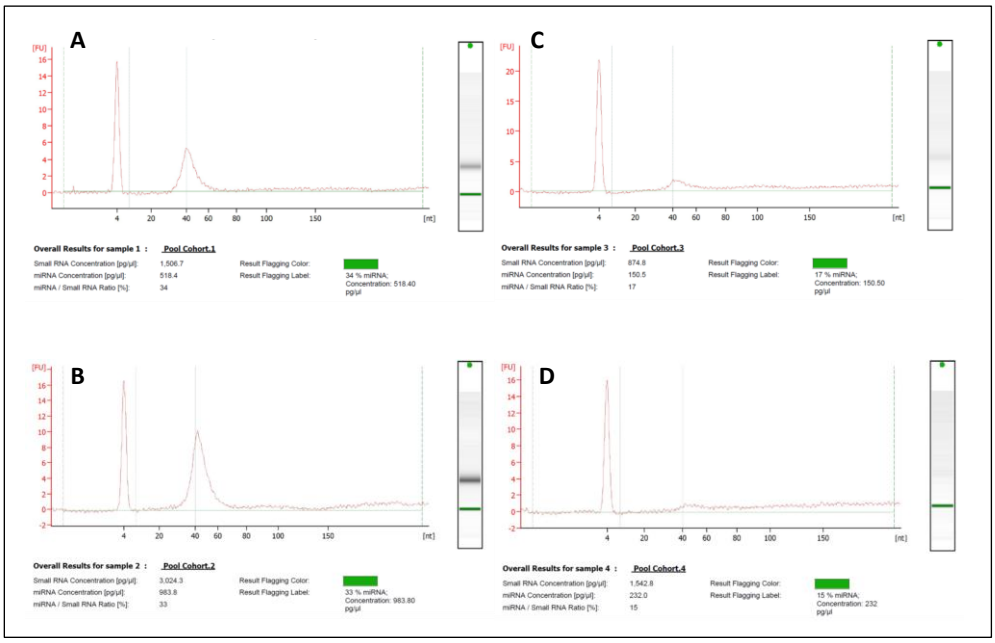

Figure 2. Plasma EV RNA quality and concentration assessed with the 2100 Bioanalyzer. (A) Cohort 1: COVID19+T2DM+; (B) Cohort 2: COVID19+T2DM-; (C) Cohort 3: RSP+T2DM+; and (D) Cohort 4: RSP+T2DM-

Differential expression analysis of circulating EV proteins

The EV proteins were further analyzed and compared by the researchers for three comparisons using linear models: the COVID-19 effect independent of diabetes background, the T2DM effect independent of acute respiratory infection type, and the T2DM-by-COVID-19 interaction effects. Tables presented in Appendixes 1-3 report on these differentially expressed EV proteins (fold change > 2, $P < 0.05$, FDR < 0.05). Further, unsupervised clustering was performed using the combined differentially expressed EV protein signatures. The previous finding with the multidimensional scaling plot was supported as the 4 study groups were successfully distinguished with close to 100% accuracy (Figure 4).

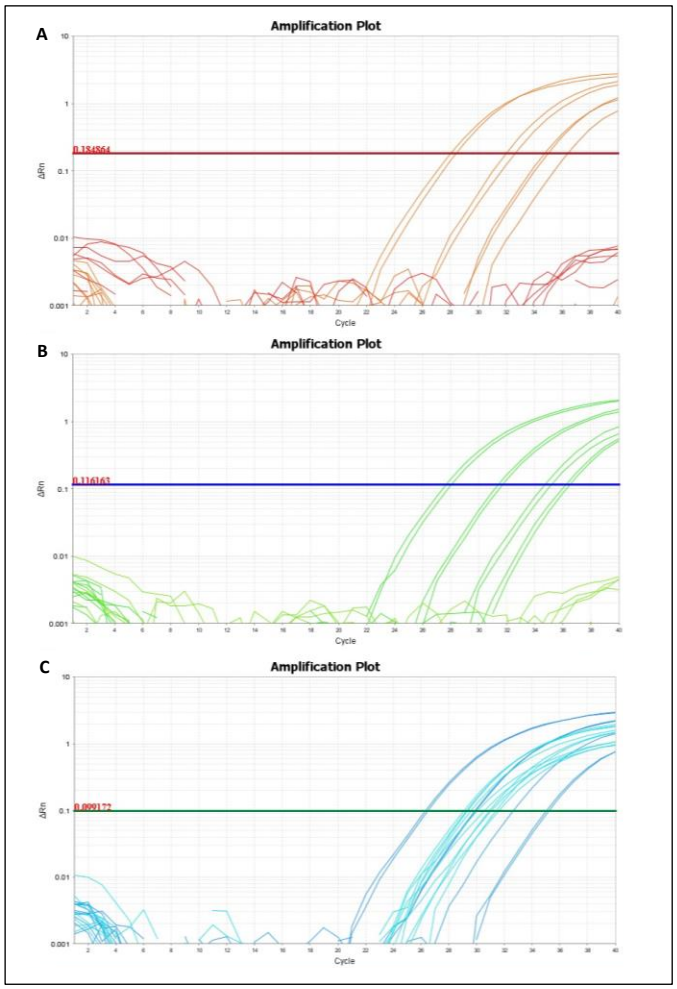

Figure 3. QPCR test for detection of COVID-19 RNA. (A) COVID-19 N1 assay, (B) COVID-19 N2 assay, (C) Human RNase-P Control Assay. Amplification curves in all assays demonstrated expected performance of the assays in the standard curve samples. Amplification curves in all samples in panel C (For the human RNase-P gene) demonstrate the amplification-suitable quality of the RNA extracted.

Functional enrichment analysis provides insight into COVID-19 and T2DM.

The researchers also conducted functional enrichment analysis to further analyze the expressed EV proteins. They detected various functional themes– represented by up- and downregulations of various proteins– that support or counter existing research findings to develop an understanding of the interaction between COVID-19 and T2DM.

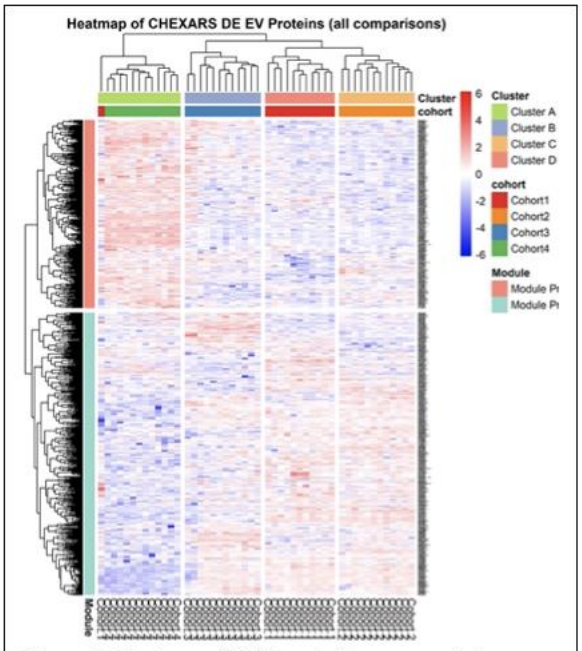

Figure 4. Heatmap of differentially expressed plasma EV proteins

For example, they detected a theme between the independent effects of COVID-19 and T2DM specific networks that revolve around the upregulation of the C1QA, C1QB, and C1QC trio of adaptive immune response complement proteins in the circulating plasma EVs (Figure 5A-C). These proteins are predominantly produced by potent antigen presenting cells such as monocytes, macrophages, and dendritic cells. These proteins have been reported to transiently attach to the cell surface and recognize danger signals (Ghebrehiwet, Hosszu, and Peerschke, 2017). They reason that the presence of the C1Q proteins on the EV surface may reflect an increase production of these molecules by a variety of activated antigen presenting cells (APC) in response to SARS-CoV-2 infection and/or diabetes. On the other hand, the C1Q+ EVs may themselves spread immuno-modulatory cargo farther away from the localized sites of APC infiltration and C1Q synthesis.

Another common functional theme between the independent effects of COVID-19 and T2DM was the significant downregulation of the central EV protein network transducer PRKCB (Figure 5D). These findings presented therapeutic options.

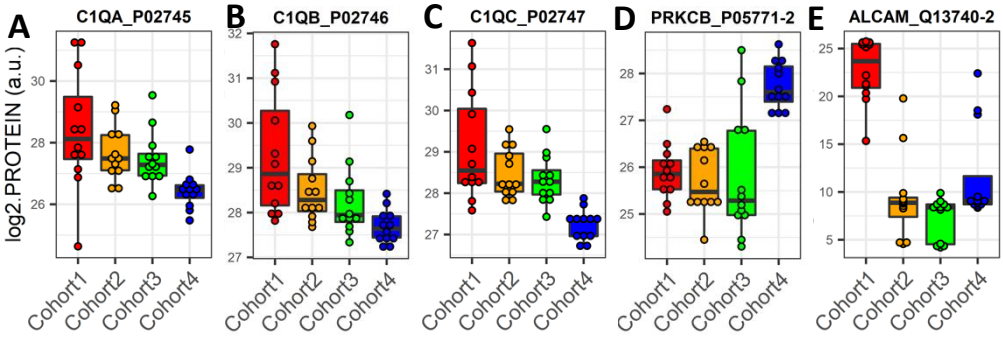

Figure 5. Networks of enriched biological processes and KEGG pathways in differentially expressed signatures of the CHEXARS study.

PRKCB is a Protein Kinase C (PKC) family member that negatively regulates mitochondrial energetics, inhibits autophagy, and also play roles in immunoreceptor and insulin receptor systems (Patergnani, S. et al., 2013). Notably, the kinase activity of PKC was found to increase within 15 minutes of SARS-CoV-2 infection and to contribute (particularly PKCβ) to viral entry into the host cell. The PKC inhibitors bisindolylmaleimide IX, sotrastaurin (an orally-active, first-in-class immunomodulator), enzastaumn, and PKCβ small interfering RNAs significantly inhibited SARS-CoV-2 replication in vitro (Liu, S. et al., 2021). Thus, our results suggest that SARS-CoV-2 infection may alter the cellular secretory pathway in order to retain kinases such as PKCβ, consequently increasing their intracellular activity while reducing their concentrations in secreted exosomes. The demonstrated role for PKCβ activity during SARS-CoV-2 entry in vitro, supported by our EV-mediated findings in infected human subjects, suggest the therapeutic utility of PKC inhibitors.

The researchers detected a highly significant COVID-19 by T2D interaction in trafficking molecule ALCAM (Figure 5E), which has been associated with SARS-CoV-2 infection in hospitalized patients and disease severity and mortality (Rébillard, R.-M. *et al.*, 2020). Because ALCAM is involved in leukocyte transendothelial migration (one of the KEGG pathways found enriched among the differentially expressed EV proteins– data not shown) and the stabilization of the immune synapse (Rébillard, R.-M. *et al.*, 2020), we reasoned that its highly elevated levels in circulating EVs from COVID-19 patients with T2D may indicate an enhanced communication activity among immune cells and the endothelium, which would contribute to the increased inflammation in these patients. These results suggest that EVs may play a central communication role contributing to the severity of COVID-19 disease.

The researchers identified several other relationships with proteins involved in inflammation and signaling that affect the progression of COVID-19 disease and further our understanding of the interaction between COVID-19 and T2DM. These findings are not discussed at length here due to being out of the scope of this thesis's aims and research.

Discussion

Altogether, our study makes an important contribution towards defining the proteomic landscape of circulating EVs in people with COVID-19 and T2DM and identifying biological mechanisms likely driving the interaction between the two diseases. Although our study is limited by a relatively small sample size, the careful selection of the study cohorts to control for confounding factors and the use of state-of-the-art methods for non-antibody-based specific EV isolation strengthen our results. Future directions include validating the current results in additional independent cohort(s) and conducting additional studies to assess the clinical utility of the suggested therapeutic targets.

Results from the nanoparticle tracking analysis and the bioanalyzer analysis provide future directions for our research. With EVs from the COVID-19 groups having increased levels of small RNAs, profiling these small noncoding RNAs (e.g., using next generation sequencing technologies such as miRNA-seq and sncRNA-seq) could shed light on their regulatory functions in the disease mechanisms of COVID-19. The fact that the increase (approximately 2-fold or 100% increase) in the amount of small RNA in the circulating EVs for the COVID-19 groups, compared to the respective controls with alternative acute respiratory disease, is dramatically larger that the increase in the concentration of plasma EVs (approximately 30% increase), suggests that EV-shuttled small noncoding RNAs may play important regulatory roles during COVID-19 development and/or progression.

The negative result of the qPCR tests does not necessarily signify the absence of the virus in our EV preparations, but rather that we could not detect viral material. These results provide future directions as other research has been able to detect SARS-CoV-2 RNA in EVs using

different methods, including more sensitive amplication-based technology known as digital PCR (Barberis, et al., 2021). An alternative explanation is that the EVtrap method employed for EV isolation in our study may be more specific for the isolation of EVs, with negligible co-isolation of viral particle contamination. This would suggest the non-existence of the hypothesized Trojan EVs carrying hidden SARS-CoV-2 virions. This alternative explanation is further supported by the fact that no viral proteins were detected by the EV proteomic analysis. However, high abundance proteins mask the identification by mass spectrometry of proteins with low abundance levels, therefore viral proteins potentially present in traces amount in the circulating EVs may have been missed due to a sensitivity issue.

Appendix

Table 2: Appendix 1. Differential EV protein expression due to the COVID-19 effect (independent of T2DM).

Uniprot	SYMBOL	logFC	AveExpr	P.Value	adj.P.Val
P31948	STIP1	-5.33	28.30	6.28E-21	8.92E-18
P02545-3	LMNA	10.45	27.99	2.68E-18	1.91E-15
P42680	TEC	-20.81	14.23	4.53E-18	2.15E-15
Q96CX2	KCTD12	-5.43	26.55	2.42E-17	8.61E-15
P51149	RAB7A	-4.36	27.02	2.39E-16	5.03E-14
Q9P289	STK26	5.64	26.08	2.42E-16	5.03E-14
Q14974	KPNB1	4.76	23.22	2.48E-16	5.03E-14
P27348	YWHAQ	7.68	27.51	3.16E-16	5.61E-14
P15291-2	B4GALT1	-3.65	24.95	3.08E-15	4.86E-13
Q86VF7-1	NRAP	-5.89	27.72	3.93E-15	5.58E-13
Q9NVA2-1	SEPTIN11	-5.02	25.21	5.13E-15	6.62E-13
P53396-2	ACLY	-5.25	26.33	5.79E-14	6.86E-12
O76074	PDE5A	4.87	28.69	1.18E-12	1.30E-10
Q8TF42	UBASH3B	4.15	24.48	2.00E-12	1.93E-10
Q13642	FHL1	-4.82	27.84	2.03E-12	1.93E-10
Q5TDH0-3	DDI2	-5.00	26.86	4.14E-12	3.68E-10
O14974-5	PPP1R12A	6.84	24.03	5.18E-12	4.33E-10
P08754	GNAI3	2.11	25.03	5.76E-12	4.54E-10
P02814	SMR3B	-12.61	19.61	2.43E-11	1.82E-09
P81605	DCD	-3.45	28.43	3.54E-11	2.52E-09
Q13472-1	TOP3A	20.37	14.06	4.01E-11	2.71E-09
P0DOX2	NA	-2.76	29.31	4.77E-11	3.08E-09
P07195	LDHB	1.86	28.23	6.21E-11	3.84E-09
Q6KB66-2	KRT80	4.41	26.73	6.55E-11	3.88E-09
Q9UIB8	CD84	3.54	24.99	1.15E-10	6.51E-09
O00712-4	NFIB	7.56	28.91	1.20E-10	6.53E-09
Q05682-4	CALD1	4.79	28.82	4.48E-10	2.36E-08
P04080	CSTB	-2.24	24.32	5.80E-10	2.94E-08
P19652	ORM2	3.39	24.78	7.56E-10	3.71E-08
Q99623	PHB2	-10.80	23.95	8.34E-10	3.95E-08
P31939	ATIC	19.03	23.64	1.12E-09	5.12E-08
Q7RTS7	KRT74	21.12	20.19	1.59E-09	7.04E-08
P05160	F13B	2.47	25.87	1.87E-09	8.05E-08
P04792	HSPB1	2.20	24.54	2.43E-09	1.02E-07
Q5JWF2-2	GNAS	-3.49	23.46	2.54E-09	1.03E-07

P52209	PGD	6.13	29.28	4.16E-09	1.64E-07
Q06033-1	ITIH3	1.44	29.54	4.38E-09	1.68E-07
Q14247-1	CTTN	-2.36	27.42	4.91E-09	1.81E-07
Q9GZU7-1	CTDSP1	-18.19	14.37	5.09E-09	1.81E-07
P01009-1	SERPINA1	-1.87	32.36	5.21E-09	1.81E-07
P23083	NA	3.42	27.99	5.30E-09	1.81E-07
P06729	CD2	-15.90	17.13	5.41E-09	1.81E-07
P33121	ACSL1	16.95	19.57	5.49E-09	1.81E-07
P25325	MPST	-18.58	17.79	7.11E-09	2.30E-07
Q6ZVX7	NCCRP1	3.56	24.08	8.34E-09	2.63E-07
P27169	PON1	1.74	29.66	1.34E-08	4.13E-07
Q08722	CD47	13.13	18.71	1.60E-08	4.83E-07
P50552	VASP	2.14	26.87	1.67E-08	4.93E-07
P29728	OAS2	17.24	16.84	1.85E-08	5.35E-07
P04843	RPN1	2.71	23.45	2.06E-08	5.87E-07
P48059	LIMS1	-2.38	27.89	2.81E-08	7.83E-07
Q13045-2	FLII	-15.41	14.23	3.57E-08	9.75E-07
P22061	PCMT1	-3.78	25.23	3.64E-08	9.75E-07
Q6UX71-1	PLXDC2	-16.28	20.88	3.82E-08	1.00E-06
P37837	TALDO1	2.07	25.05	4.18E-08	1.08E-06
P48426	PIP4K2A	-9.51	11.37	4.34E-08	1.10E-06
P29401	TKT	-2.23	24.76	4.94E-08	1.23E-06
P20042	EIF2S2	-16.25	14.77	5.23E-08	1.28E-06
P23919	DTYMK	15.15	13.31	5.70E-08	1.37E-06
Q9NRW1	RAB6B	-4.44	24.98	6.01E-08	1.42E-06
Q01546	KRT76	-12.26	23.89	6.13E-08	1.43E-06
P11413-3	G6PD	2.24	28.61	6.54E-08	1.50E-06
A0A0B4J1X5	NA	-4.58	25.20	6.92E-08	1.56E-06
P05534	NA	1.77	28.09	7.96E-08	1.77E-06
O43294-1	TGFB1I1	-2.42	24.42	8.42E-08	1.84E-06
Q14520-1	HABP2	2.13	29.70	8.81E-08	1.88E-06
P41218	MNDA	-12.79	23.30	8.84E-08	1.88E-06
P01011-1	SERPINA3	2.26	30.13	9.30E-08	1.94E-06
P49748-1	ACADVL	12.79	24.09	9.84E-08	2.03E-06
Q08495-1	DMTN	3.88	28.85	1.01E-07	2.04E-06
Q68BL7-2	OLFML2A	14.45	17.81	1.12E-07	2.24E-06
P62158	NA	1.54	27.19	1.14E-07	2.25E-06
P28074-1	PSMB5	-4.06	24.34	1.16E-07	2.27E-06
Q96P48-6	ARAP1	-19.64	14.09	1.23E-07	2.36E-06
P19013	NA	-2.03	28.77	1.27E-07	2.39E-06

O15117-3	FYB1	-2.31	26.42	1.29E-07	2.39E-06
P11277	SPTB	-1.37	30.38	1.30E-07	2.39E-06
P40926	MDH2	2.16	25.49	1.41E-07	2.57E-06
P08311	CTSG	-2.35	25.11	1.69E-07	3.01E-06
Q14677-3	CLINT1	5.47	24.28	1.70E-07	3.01E-06
P05091	ALDH2	-12.51	11.88	1.72E-07	3.01E-06
Q13740-2	ALCAM	14.12	14.29	1.92E-07	3.33E-06
P00450	CP	-1.24	30.27	2.91E-07	4.98E-06
P53814-1	SMTN	-14.55	15.70	3.02E-07	5.11E-06
O15144	ARPC2	2.17	27.78	3.20E-07	5.36E-06
Q13576-1	IQGAP2	-1.96	28.74	3.66E-07	6.05E-06
O94804	STK10	4.62	27.81	3.98E-07	6.49E-06
P00740	F9	-1.36	27.01	4.73E-07	7.64E-06
Q9C075	KRT23	-2.88	23.55	4.93E-07	7.87E-06
O75923-3	DYSF	3.10	26.14	5.28E-07	8.34E-06
Q9H0U4	RAB1B	1.14	26.22	5.99E-07	9.36E-06
Q08554-2	DSC1	-1.47	27.83	6.95E-07	1.07E-05
Q99972	MYOC	-16.62	17.73	7.04E-07	1.07E-05
P62258-1	YWHAE	-2.38	28.28	7.10E-07	1.07E-05
P11279	LAMP1	-15.66	15.75	8.00E-07	1.20E-05
O60925	PFDN1	9.43	10.97	9.87E-07	1.46E-05
P29350-3	PTPN6	2.07	25.90	1.14E-06	1.67E-05
P53990-5	IST1	-5.08	24.38	1.32E-06	1.92E-05
P07384	CAPN1	-2.11	26.29	1.37E-06	1.97E-05
A0A075B6I1	NA	16.02	17.86	1.45E-06	2.07E-05
P49593	PPM1F	-11.71	20.46	1.53E-06	2.13E-05
P51606-1	RENBP	4.26	25.73	1.53E-06	2.13E-05
P01721	NA	12.64	12.54	1.58E-06	2.18E-05
O75347	TBCA	-15.59	16.62	1.60E-06	2.18E-05
Q9Y266	NUDC	-16.40	14.91	1.66E-06	2.25E-05
Q92764	KRT35	-16.50	14.62	1.73E-06	2.32E-05
Q13287	NMI	-10.75	14.31	1.89E-06	2.51E-05
Q96L93-1	KIF16B	-1.41	27.35	2.02E-06	2.66E-05
P30046	DDT	14.64	16.70	2.20E-06	2.86E-05
P08865	RPSA	-15.55	15.47	2.23E-06	2.88E-05
P14770	GP9	-1.33	27.57	2.61E-06	3.34E-05
P08238	HSP90AB1	-1.84	25.66	2.66E-06	3.35E-05
P04279-1	SEMG1	-13.58	16.34	2.66E-06	3.35E-05
Q7L7X3	TAOK1	-4.28	22.00	3.42E-06	4.27E-05
P01019	AGT	2.41	25.43	3.82E-06	4.72E-05

P48643	CCT5	-2.10	25.74	4.14E-06	5.07E-05
Q9H444	CHMP4B	-2.08	26.10	4.23E-06	5.14E-05
Q6ZUX7	LHFPL2	-13.16	21.13	4.31E-06	5.19E-05
P61981	YWHAG	-1.48	26.47	4.35E-06	5.19E-05
P08253-3	MMP2	-2.59	23.96	4.42E-06	5.23E-05
P13498	CYBA	11.11	11.60	4.87E-06	5.70E-05
P50851-1	LRBA	3.21	24.13	4.92E-06	5.70E-05
O75342	ALOX12B	3.03	24.40	4.93E-06	5.70E-05
Q5D862	FLG2	-1.98	27.20	5.27E-06	6.04E-05
Q9UPN3	MACF1	2.44	26.42	5.53E-06	6.28E-05
P00451	F8	-2.16	24.82	5.76E-06	6.49E-05
P20062-1	TCN2	12.96	12.49	7.31E-06	8.18E-05
O75015	FCGR3B	-4.36	23.50	7.86E-06	8.68E-05
P26572	MGAT1	-2.60	26.39	7.88E-06	8.68E-05
P00739-1	HPR	1.80	27.83	8.23E-06	9.00E-05
P00747	PLG	1.03	30.99	8.34E-06	9.04E-05
P02730	SLC4A1	1.62	30.77	8.63E-06	9.24E-05
O00161	SNAP23	-1.46	25.46	8.64E-06	9.24E-05
P12268	IMPDH2	-13.51	14.08	8.80E-06	9.34E-05
P02747	C1QC	2.31	29.44	8.93E-06	9.40E-05
Q13492-1	PICALM	-11.79	17.69	9.72E-06	0.000101556
P33176	KIF5B	-11.01	18.58	9.82E-06	0.000101688
P22392-2	NME2	1.19	25.08	9.90E-06	0.000101688
P30626-1	SRI	2.18	24.46	9.95E-06	0.000101688
P00367	GLUD1	-14.51	15.34	1.08E-05	0.000109511
P07357	C8A	-1.59	28.60	1.14E-05	0.000114451
Q9Y6E0	STK24	2.33	25.87	1.14E-05	0.000114451
P30273	FCER1G	2.19	25.63	1.17E-05	0.000116463
Q01629	IFITM2	9.84	21.63	1.20E-05	0.000118001
Q9NYL9	TMOD3	2.18	24.91	1.56E-05	0.000152538
Q04695	KRT17	-2.07	27.04	1.57E-05	0.000152538
O75083	WDR1	1.11	28.15	1.60E-05	0.000155043
Q9UBV8	PEF1	-14.71	12.76	1.70E-05	0.000163233
P48594	SERPINB4	-14.43	15.81	1.71E-05	0.000163543
Q9UL46	PSME2	3.48	23.60	1.76E-05	0.000164729
P13929-1	ENO3	11.92	18.32	1.76E-05	0.000164729
P00558	PGK1	1.03	26.65	1.76E-05	0.000164729
P14314-2	PRKCSH	-2.57	23.64	1.81E-05	0.000168491
Q08830	FGL1	2.65	25.92	1.84E-05	0.000169633
Q8NEY1-3	NAV1	2.30	29.52	1.92E-05	0.000175631

P31146	CORO1A	-1.50	26.92	1.98E-05	0.000180772
P05771-2	PRKCB	-2.25	25.43	2.08E-05	0.000188518
P01023	A2M	-1.01	32.00	2.13E-05	0.000191132
P09497-1	CLTB	-2.12	23.23	2.40E-05	0.000213714
P62136-1	PPP1CA	-2.46	24.24	2.41E-05	0.000213714
Q9H479	FN3K	6.24	23.97	2.44E-05	0.000214953
P0DMV8	HSPA1A	1.15	25.47	2.47E-05	0.00021606
Q03164	KMT2A	1.84	28.80	2.48E-05	0.00021606
P22352	GPX3	2.84	27.09	2.61E-05	0.000225761
P02748	C9	1.22	31.72	2.66E-05	0.000228356
Q96BY6-3	DOCK10	3.34	26.06	2.67E-05	0.000228356
P61769	B2M	1.63	26.26	2.70E-05	0.000229988
Q96QA5	GSDMA	2.11	24.13	2.84E-05	0.000240421
P20742	NA	-1.42	26.48	2.88E-05	0.000242301
P51809	VAMP7	-9.17	11.25	2.92E-05	0.000243773
Q9BXR6	CFHR5	-2.00	26.51	3.26E-05	0.000270508
P25705-1	ATP5F1A	1.39	25.01	3.36E-05	0.000277746
Q9UKV8	AGO2	8.57	23.81	3.41E-05	0.000279706
P11766	ADH5	-12.25	17.47	3.55E-05	0.000288387
P23229-6	ITGA6	-1.50	27.49	3.58E-05	0.000288387
P07814	EPRS1	-11.35	11.79	3.58E-05	0.000288387
P30043	BLVRB	1.58	25.91	3.59E-05	0.000288387
P15907	ST6GAL1	-2.47	24.14	3.67E-05	0.000292903
Q06187	BTK	-2.05	23.52	3.71E-05	0.000294452
P01717	NA	2.19	27.91	3.75E-05	0.000295819
O14791-2	APOL1	1.30	29.50	4.12E-05	0.0003231
O43639	NCK2	-2.29	23.46	4.48E-05	0.000348235
Q9UQP3	TNN	12.48	20.43	4.53E-05	0.000349587
Q00577	PURA	-9.21	11.22	4.70E-05	0.000360829
P05155-3	SERPING1	1.74	28.75	4.90E-05	0.000374271
P48444	ARCN1	-8.44	11.15	5.34E-05	0.00040584
Q9Y696	CLIC4	-1.64	25.37	5.52E-05	0.000417471
Q93084	ATP2A3	1.15	25.47	5.93E-05	0.000445579
P08631-4	HCK	11.57	20.27	5.96E-05	0.000445579
P01619	NA	7.78	23.43	6.04E-05	0.000449648
P18206-2	VCL	-1.17	30.80	6.10E-05	0.000451132
Q14315	FLNC	-13.44	18.05	6.27E-05	0.000461182
O75563	SKAP2	-2.14	24.79	6.30E-05	0.000461182
Q9ULP9	TBC1D24	-4.10	25.11	6.93E-05	0.000502337
P02753	RBP4	1.41	27.41	7.02E-05	0.000506428

O60240	PLIN1	2.64	24.66	7.26E-05	0.000521109
Q8NEU8-1	APPL2	-13.86	15.09	8.41E-05	0.000600682
P00748	F12	1.20	26.40	8.46E-05	0.000600856
Q96Q06-1	NA	-5.52	24.63	8.56E-05	0.000602709
Q15102	PAFAH1B3	11.81	14.01	8.57E-05	0.000602709
Q6E0U4-6	DMKN	1.80	23.55	8.96E-05	0.000627106
P21266	GSTM3	13.93	16.64	9.25E-05	0.000644487
P33151	CDH5	-2.28	25.53	9.71E-05	0.000673326
Q9C0H2-1	TTYH3	-10.79	13.29	0.000103105	0.000711227
P09769	FGR	10.43	18.61	0.000104371	0.000716481
Q13464	ROCK1	-11.60	14.58	0.000113519	0.000772355
P06858	LPL	-11.09	12.80	0.000113598	0.000772355
P20851	C4BPB	-1.56	28.27	0.000116792	0.000790289
P27824	CANX	1.16	25.32	0.000117495	0.00079128
Q9NQ79	CRTAC1	1.85	24.08	0.000121974	0.000817574
P22694-1	PRKACB	-11.23	19.85	0.000125095	0.000834553
P24821	TNC	-1.78	23.32	0.000125741	0.000834946
Q9ULA0	DNPEP	-13.21	16.66	0.000137352	0.000905303
Q15819	UBE2V2	1.55	23.47	0.000137949	0.000905303
Q8NF91-7	SYNE1	1.26	26.15	0.000138248	0.000905303
O15400-2	STX7	1.79	26.22	0.000145256	0.000936417
Q9Y6Z7	COLEC10	2.48	25.57	0.000145275	0.000936417
Q04760-1	GLO1	12.56	13.20	0.000145636	0.000936417
P12273	PIP	2.93	25.71	0.000149105	0.000954406
Q8IZ83	ALDH16A1	-2.53	24.75	0.000155064	0.000983689
P01742	NA	-1.46	27.06	0.000160462	0.001012846
P04839	CYBB	-8.59	19.88	0.000161086	0.001012846
P0C869	JMJD7-PLA2G4B	-10.65	11.91	0.000166879	0.001044647
O75636-1	FCN3	1.28	27.94	0.000174088	0.001084998
P08758	ANXA5	1.99	24.03	0.000186185	0.001150298
P04196	HRG	1.42	27.89	0.000194475	0.001196314
P07900-2	HSP90AA1	-2.02	27.82	0.000196844	0.001205667
P37840-1	SNCA	1.65	27.02	0.000208716	0.001272897
P10720	PF4V1	-1.33	28.65	0.000219403	0.001332358
P07996	THBS1	-1.14	30.04	0.000261097	0.001578802
Q15365	PCBP1	-1.51	26.00	0.000265031	0.001595802
Q99952	PTPN18	-10.75	21.11	0.000269448	0.001615549
P02746	C1QB	2.07	29.08	0.000290453	0.001726919
Q9BR76	CORO1B	5.55	23.45	0.000296441	0.001755177
Q3V6T2-1	CCDC88A	-1.76	25.24	0.000298204	0.001758289

P11021	HSPA5	-1.45	27.31	0.000304763	0.001789536
P50453	SERPINB9	5.52	21.13	0.000310482	0.001815619
Q9UBW5-1	BIN2	1.24	27.40	0.000318945	0.001857462
P13667	PDIA4	2.25	24.23	0.000325855	0.001889959
O75791	GRAP2	3.44	22.79	0.000356249	0.002057846
Q5QNW6-1	H2BC18	4.18	24.52	0.0003697	0.002114781
P30085-1	CMPK1	-1.96	23.15	0.00037057	0.002114781
P01860	NA	1.84	30.97	0.000393805	0.002238389
Q00796	SORD	6.63	10.62	0.000396045	0.002240354
Q4LDE5	SVEP1	-1.27	26.80	0.000397304	0.002240354
Q5SW79-1	CEP170	1.83	24.79	0.000399217	0.002242244
Q4KMP7	TBC1D10B	1.86	24.22	0.000402584	0.002252253
Q9HCS7	XAB2	-1.20	29.46	0.000408955	0.00227892
P13797	PLS3	10.67	17.41	0.000411506	0.002281538
Q06830	PRDX1	1.15	27.12	0.000417062	0.002297072
P55160	NCKAP1L	-7.65	21.20	0.000435662	0.002390252
Q8IVB4	SLC9A9	-8.96	18.96	0.000447748	0.002447114
P62330	ARF6	10.39	17.77	0.000450112	0.002450609
Q9UNS2	COPS3	10.81	21.74	0.000457068	0.002478984
P07360	C8G	-2.08	26.57	0.000460395	0.002487534
P06331	NA	1.51	28.08	0.000464679	0.002496784
P61088	UBE2N	-1.24	24.76	0.00046617	0.002496784
P31323	PRKAR2B	-9.74	12.03	0.000467378	0.002496784
P27797	CALR	-1.33	25.46	0.000482605	0.002568468
P08185	SERPINA6	1.44	25.27	0.000494696	0.002605099
Q13404	UBE2V1	9.19	17.41	0.000495284	0.002605099
O15498	YKT6	11.36	14.77	0.000495677	0.002605099
P62851	RPS25	-9.67	15.63	0.000529604	0.00276679
P42574	CASP3	6.62	25.44	0.00055681	0.002891674
Q13103	SPP2	1.01	28.61	0.000577782	0.002985556
O43396	TXNL1	3.09	23.88	0.000588009	0.003027393
Q9BXN1	ASPN	2.22	23.86	0.000616555	0.003162906
Q6PKX4	DOK6	-2.08	27.51	0.000622919	0.00318191
P01034	CST3	-2.11	26.23	0.000624738	0.00318191
Q13835	PKP1	3.48	26.76	0.000635498	0.00322515
Q9NTJ5	SACM1L	1.91	25.57	0.000658833	0.00333168
P42357	HAL	8.12	21.51	0.000663031	0.003341016
Q9NQW7-1	XPNPEP1	-10.35	14.27	0.000705153	0.003539206
O75558	STX11	1.65	23.35	0.000707343	0.003539206
Q99832	CCT7	1.24	25.48	0.000716597	0.003564422

O15056	SYNJ2	-1.56	27.07	0.000717399	0.003564422
O15078-1	CEP290	1.23	29.97	0.000720716	0.003568422
P12883	MYH7	2.32	23.84	0.000742065	0.003652707
P80723	BASP1	-2.43	26.29	0.00074288	0.003652707
P06239-1	LCK	-10.13	11.93	0.000779671	0.003820388
E9PAV3	NA	11.66	17.94	0.000791567	0.003865351
Q15836	VAMP3	11.53	15.89	0.000819619	0.003979233
Q07812	BAX	7.01	12.04	0.000840205	0.004060989
Q14525	KRT33B	-7.54	19.91	0.000865286	0.004168037
O95436-1	SLC34A2	11.21	16.27	0.000868451	0.00416915
Q8N699	MYCT1	-5.86	22.57	0.000872659	0.004175246
Q9Y4F9	RIPOR2	-6.30	22.11	0.000886708	0.004228229
Q5VY43	PEAR1	9.76	12.96	0.000889813	0.004228846
P68371	TUBB4B	-1.22	27.54	0.000898991	0.004258221
O14818-2	PSMA7	-2.94	26.24	0.000946587	0.004453972
Q5JSH3	WDR44	1.84	24.84	0.000949861	0.004454627
P07093-1	SERPINE2	-9.40	19.28	0.000979198	0.004577109
P30536	TSPO	11.00	13.96	0.001033939	0.004817139
P43487	RANBP1	1.91	24.06	0.001045957	0.004857206
Q5VST9-6	OBSCN	-2.09	27.03	0.00107805	0.004989934
O95721	SNAP29	6.96	19.05	0.001103275	0.005087089
Q9NRY5	FAM114A2	-5.15	11.71	0.001109011	0.005087089
Q8WUA8	TSKU	6.05	23.35	0.001111974	0.005087089
P61106	RAB14	1.50	26.75	0.00111336	0.005087089
P80511	S100A12	10.17	17.46	0.001121681	0.005100029
P21281	ATP6V1B2	-3.14	23.63	0.001126959	0.005100029
P14543-1	NID1	1.73	24.76	0.001160644	0.005235792
P50402	EMD	-10.72	15.65	0.001170341	0.005262831
Q6BDS2	UHRF1BP1	9.31	20.29	0.001206115	0.005402473
P45974-1	USP5	1.32	23.84	0.001330155	0.005905126
Q9HB21-1	PLEKHA1	-1.32	29.29	0.001333952	0.005905126
P04075	ALDOA	-1.01	27.80	0.001383237	0.006085385
O14950	MYL12A	1.48	23.01	0.001395934	0.006122289
P02745	C1QA	2.39	27.92	0.001445605	0.00630124
P01714	NA	2.39	26.51	0.001546615	0.006720918
Q8N6C8-3	LILRA3	-6.07	23.18	0.001561906	0.006766673
P08648	ITGA5	1.20	23.09	0.001598311	0.006903345
P01591	JCHAIN	1.52	28.84	0.001607088	0.006904983
P19634-1	SLC9A1	11.06	16.45	0.001608409	0.006904983
P16070-7	CD44	-1.55	23.83	0.001616958	0.006920773

Q02108	GUCY1A1	-9.20	14.04	0.001653747	0.007056979
Q16881-1	TXNRD1	9.34	15.16	0.001663807	0.007062877
P58335-1	ANTXR2	9.44	13.97	0.00166626	0.007062877
P61006	RAB8A	-1.17	24.26	0.00167004	0.007062877
P35606	COPB2	5.86	18.81	0.001787426	0.007499521
P01859	NA	1.73	27.28	0.001788542	0.007499521
P01137	TGFB1	-1.03	25.65	0.001789119	0.007499521
Q08188	TGM3	-1.68	26.64	0.001869646	0.007787924
Q96KP4	CNDP2	3.07	24.32	0.001874363	0.007787924
O43561	LAT	-1.07	23.13	0.001946636	0.008041191
P29508	SERPINB3	1.59	26.63	0.002013683	0.008294041
Q6UY14-1	ADAMTSL4	6.65	20.32	0.002020932	0.008299841
P43250-2	GRK6	-9.84	13.29	0.002037897	0.008345392
P11234-2	RALB	1.57	25.44	0.002090397	0.008535789
P20700	LMNB1	-7.91	13.19	0.002113904	0.008588261
O75964	ATP5MG	8.00	21.22	0.002115335	0.008588261
P48507	GCLM	4.64	22.63	0.002135987	0.008647401
P36955	SERPINF1	-2.31	26.26	0.002162348	0.008729251
O14633	LCE2B	5.64	20.50	0.002224964	0.008956581
Q9P126	CLEC1B	-2.53	24.89	0.002278087	0.009144522
P55259-1	GP2	9.14	14.42	0.002439023	0.009762962
Q01813	PFKP	1.09	24.95	0.002591011	0.010313241
Q9UQ80	PA2G4	-2.11	25.46	0.002709731	0.010755665
P01782	NA	-1.68	23.76	0.002806782	0.011037629
P09543-1	CNP	1.06	25.85	0.002809747	0.011037629
P48739	PITPNB	9.32	13.22	0.002810374	0.011037629
Q8WWA0	ITLN1	8.05	20.01	0.002811838	0.011037629
P78527	PRKDC	2.45	27.74	0.002842891	0.011128781
Q96F07	CYFIP2	-1.79	24.37	0.002939682	0.011444625
Q71U36	TUBA1A	11.05	19.58	0.002962986	0.011503835
P26927	MST1	5.38	21.70	0.002991544	0.011583061
P50990	CCT8	1.27	25.62	0.003121242	0.012033915
P52306-6	RAP1GDS1	-9.80	13.43	0.003124922	0.012033915
Q9BZQ8	NIBAN1	8.45	18.56	0.003205918	0.012312457
P62491-1	RAB11A	1.21	26.68	0.003395406	0.013005044
Q13421	MSLN	8.45	16.17	0.003471796	0.013261886
Q8TE73	DNAH5	-9.85	13.47	0.00355018	0.013488787
P00492	HPRT1	-4.26	22.83	0.003602989	0.013652926
Q14642	INPP5A	8.55	18.52	0.003750915	0.014175667
P38646	HSPA9	2.56	21.35	0.003789943	0.014285168

Q15758-1	SLC1A5	-8.51	12.73	0.003951426	0.01481524
P35612-1	ADD2	1.18	25.32	0.004093746	0.015308457
Q9H2K8	TAOK3	1.08	25.13	0.004136338	0.015427129
Q15642	TRIP10	-7.92	13.87	0.004175344	0.015531842
Q8WWA1-2	TMEM40	-9.07	18.52	0.004231724	0.015659582
Q92973-1	TNPO1	9.92	20.64	0.004333275	0.01595229
P78559-1	MAP1A	-6.74	11.11	0.004390396	0.016120808
Q9NY33-4	DPP3	8.78	17.91	0.004439855	0.016218596
A0A0C4DH31	NA	7.07	21.96	0.004600855	0.016763626
Q6UWP8-1	SBSN	2.49	27.51	0.004631056	0.016830514
Q13126-2	MTAP	1.74	26.23	0.004761831	0.017130535
P0DJI8	SAA1	1.95	29.45	0.004788332	0.017140385
O43768-3	ENSA	-9.31	14.00	0.004794284	0.017140385
P15311	EZR	-1.65	23.85	0.004800755	0.017140385
Q00013-1	MPP1	1.24	27.56	0.004835368	0.017157841
Q96SB3	PPP1R9B	-9.37	13.79	0.004853158	0.017157841
P57737-3	CORO7	-7.65	13.60	0.004853942	0.017157841
O75882-1	ATRN	6.43	22.14	0.004967921	0.017517161
P14317	HCLS1	-1.59	22.89	0.005190862	0.018212877
Q9Y6W5	WASF2	-9.81	17.09	0.005283706	0.018492971
Q15166	PON3	1.56	25.93	0.005332427	0.018617637
Q16891	IMMT	-6.17	12.86	0.005410907	0.018785348
Q14012	CAMK1	10.63	14.19	0.005420122	0.018785348
P22234	PAICS	-1.41	24.10	0.005456793	0.018820638
P23142-4	NA	3.51	21.56	0.00557809	0.019084518
Q7LDG7-2	RASGRP2	-1.54	25.21	0.00557979	0.019084518
O75832	PSMD10	-5.78	11.50	0.005594245	0.019084518
P30086	PEBP1	1.64	25.98	0.005597624	0.019084518
P12110	COL6A2	-1.11	24.25	0.005614668	0.019087184
P43034	PAFAH1B1	7.21	26.20	0.005678195	0.019257077
O95428-5	PAPLN	-9.12	14.50	0.00587603	0.019880567
P61081	UBE2M	-8.41	17.53	0.005901056	0.019917817
Q9BV40	VAMP8	-3.65	22.57	0.005941145	0.020005608
P09326	CD48	-9.24	18.77	0.006139544	0.02059167
Q9NR46	SH3GLB2	8.67	16.05	0.006144172	0.02059167
P51692	STAT5B	6.08	20.65	0.006239872	0.020863196
Q9UJU6-1	DBNL	-1.23	24.84	0.006256967	0.020871243
P07766	CD3E	9.43	17.88	0.006331004	0.021068752
Q7L9L4	MOB1B	7.81	17.54	0.006377146	0.02117272
Q15008	PSMD6	-8.07	18.39	0.006467309	0.0213722

Q02818	NUCB1	6.02	23.28	0.006832874	0.022475726
P46734-1	MAP2K3	-8.71	15.51	0.006921593	0.022714973
P04430	NA	4.90	20.81	0.006980469	0.022855405
P07339	CTSD	1.38	25.39	0.007075588	0.023113588
Q8N9U0	TC2N	6.50	14.38	0.007166813	0.023357892
P01715	NA	4.87	22.93	0.007289141	0.023702217
Q9H4F8-2	SMOC1	8.21	16.40	0.007376894	0.0239328
P24557-3	TBXAS1	1.25	24.29	0.00742133	0.024018286
Q9NTK5-1	OLA1	5.12	20.28	0.007437048	0.024018286
Q13094	LCP2	-1.37	23.52	0.007712938	0.024852801
Q9H939-1	PSTPIP2	3.10	26.77	0.007849295	0.02523495
Q15722	LTB4R	6.74	22.19	0.007940688	0.025471145
Q9H223	EHD4	-1.25	23.08	0.00822882	0.026276748
P02810	PRH1	-1.88	21.12	0.008298135	0.026438676
O95967	EFEMP2	7.13	20.29	0.008502631	0.027029618
P05154	SERPINA5	-1.34	22.81	0.008740124	0.027722581
P07451	CA3	-8.35	15.13	0.008927981	0.028255368
Q9H2G2-2	SLK	5.86	24.24	0.009003531	0.028431149
Q70J99-1	UNC13D	1.06	24.00	0.009206048	0.029006197
Q15366-3	PCBP2	-1.71	24.04	0.00923816	0.029042977
P63167	DYNLL1	5.86	21.55	0.009381156	0.029427425
P09104	ENO2	-1.93	22.40	0.009669505	0.030265124
P01701	NA	4.02	23.84	0.009830598	0.030701713
P05107	ITGB2	1.27	27.36	0.009867994	0.030750921
Q15828	CST6	-1.08	23.11	0.009909609	0.03081303
A0A0B4J1V0	NA	1.32	26.86	0.009986982	0.030985811
O00231	PSMD11	8.44	18.67	0.010042608	0.031090513
Q86UF1	TSPAN33	-9.23	16.40	0.010083855	0.031150345
Q8N4C8-3	MINK1	2.78	21.64	0.010269661	0.031592391
Q96RT1	ERBIN	-5.60	19.83	0.010271418	0.031592391
P09525	ANXA4	-7.98	13.14	0.010535371	0.032264573
P04070	PROC	1.33	24.02	0.010883056	0.033257681
P28066-1	PSMA5	-1.22	24.41	0.01095969	0.033419998
P27701	CD82	-6.29	20.61	0.011266919	0.03428328
P15814	IGLL1	5.32	22.33	0.011520979	0.034981435
P68036	UBE2L3	-7.45	15.50	0.011686932	0.035334319
P55957-1	BID	-5.48	18.11	0.011960241	0.036007419
P05164-2	MPO	-1.20	26.87	0.012504594	0.037566655
Q86UD1	OAF	5.61	20.34	0.013091696	0.039247468
Q8WV44-1	TRIM41	4.49	19.42	0.013160835	0.039371678

P38606	ATP6V1A	-4.61	21.47	0.013226138	0.039483913
Q6UWL2	SUSD1	7.12	19.68	0.013428951	0.040005324
Q92520	FAM3C	8.25	15.19	0.013772044	0.040941579
Q9UGM5-1	FETUB	1.77	27.34	0.014173941	0.041829878
P22626	HNRNPA2B1	3.73	10.52	0.014188454	0.041829878
P29966	MARCKS	1.67	24.89	0.014247474	0.041829878
Q14574-2	DSC3	9.14	17.63	0.01439953	0.042102328
Q7Z4W1	DCXR	2.62	22.39	0.014432932	0.042113339
P29622	SERPINA4	1.06	26.04	0.014568051	0.042362924
Q9Y3A6-1	TMED5	6.85	22.16	0.014578093	0.042362924
P30566	ADSL	-1.97	22.13	0.01466861	0.042527928
P06703	S100A6	-1.42	25.20	0.014694731	0.042527928
P20645	M6PR	7.26	15.40	0.014849311	0.04288795
A0M8Q6	NA	4.13	20.93	0.015039221	0.043312892
P25787	PSMA2	1.39	23.62	0.015057402	0.043312892
Q9NVJ2	ARL8B	7.32	16.38	0.015200695	0.043636744
Q15582	TGFBI	1.24	24.58	0.015431897	0.044122186
P35580-2	MYH10	1.30	26.85	0.015770928	0.0449108
Q14008	CKAP5	7.47	13.56	0.015932208	0.045279334
O95197-2	RTN3	-2.13	21.94	0.01606132	0.045536791
P40763	STAT3	-1.85	21.71	0.016135544	0.045583714
P06730	EIF4E	5.83	13.23	0.016172598	0.045597741
P19012	KRT15	2.34	21.88	0.016426554	0.04619352
P49407-1	ARRB1	4.49	21.41	0.016525441	0.046263144
Q08431	MFGE8	-5.74	19.98	0.016636568	0.046445114
P40939	HADHA	5.33	13.93	0.017040363	0.047386215
P30405	PPIF	-5.11	11.53	0.017649068	0.048887573
Q9NPQ8	RIC8A	-4.53	10.84	0.01782176	0.049269885

Table 3: Appendix 2. Differential EV protein expression due to the T2DM effect (independent of acute respiratory infection type).

Uniprot	SYMBOL	logFC	AveExpr	P.Value	adj.P.Val
Q8N1N4	KRT78	-5.42	28.63	6.59E-18	9.36E-15
Q96CX2	KCTD12	-5.22	26.55	1.77E-16	1.26E-13
P15291-2	B4GALT1	-3.60	24.95	9.56E-15	4.53E-12
P42680	TEC	-16.64	14.23	1.53E-14	5.43E-12
Q9NVA2-1	SEPTIN11	-4.67	25.21	9.43E-14	2.68E-11
Q9H444	CHMP4B	-4.20	26.10	3.31E-13	7.83E-11
P22061	PCMT1	-5.55	25.23	3.05E-12	6.20E-10
P14770	GP9	-2.23	27.57	3.04E-11	5.40E-09
Q13642	FHL1	-4.36	27.84	6.16E-11	9.73E-09
P19013	NA	-2.81	28.77	8.43E-11	1.20E-08
Q14247-1	CTTN	-2.74	27.42	1.92E-10	2.35E-08
O15400-2	STX7	3.66	26.22	1.99E-10	2.35E-08
P05160	F13B	2.68	25.87	4.06E-10	4.44E-08
P02814	SMR3B	-11.43	19.61	5.67E-10	5.76E-08
Q9HCS7	XAB2	2.53	29.46	7.15E-10	6.78E-08
Q99623	PHB2	-10.80	23.95	1.38E-09	1.18E-07
P21741	MDK	-19.49	16.50	1.41E-09	1.18E-07
P26572	MGAT1	-3.83	26.39	4.62E-09	3.65E-07
Q86TH1	ADAMTSL2	-3.74	25.69	8.59E-09	6.43E-07
P0DOX2	NA	2.26	29.31	1.13E-08	8.06E-07
O43294-1	TGFB1I1	-2.64	24.42	1.91E-08	1.26E-06
P29350-3	PTPN6	2.57	25.90	2.00E-08	1.26E-06
P10809	HSPD1	4.87	26.31	2.03E-08	1.26E-06
Q5TDH0-3	DDI2	-3.66	26.86	2.17E-08	1.28E-06
Q13586	STIM1	5.23	28.36	3.60E-08	2.04E-06
Q15149-7	PLEC	3.23	28.23	5.30E-08	2.90E-06
P48426	PIP4K2A	-9.59	11.37	5.70E-08	2.98E-06
Q9UIB8	CD84	2.79	24.99	5.87E-08	2.98E-06
O15117-3	FYB1	-2.43	26.42	6.82E-08	3.34E-06
P01011-1	SERPINA3	2.30	30.13	1.06E-07	5.02E-06
Q13404	UBE2V1	-15.83	17.41	1.20E-07	5.49E-06
P52209	PGD	5.37	29.28	1.29E-07	5.75E-06
Q9NRY5	FAM114A2	-9.51	11.71	1.34E-07	5.77E-06
P05067-1	APP	-15.77	18.29	1.85E-07	7.73E-06
Q9H299	SH3BGRL3	-4.58	24.77	2.29E-07	9.29E-06
P07307	ASGR2	16.97	12.90	2.38E-07	9.29E-06
P23467	PTPRB	-10.76	23.37	2.42E-07	9.29E-06

P62851	RPS25	-16.17	15.63	2.48E-07	9.29E-06
Q14677-3	CLINT1	5.44	24.28	2.81E-07	1.02E-05
P49908	SELENOP	1.69	28.37	3.02E-07	1.07E-05
Q13287	NMI	-11.99	14.31	3.42E-07	1.19E-05
Q07960	ARHGAP1	-3.85	25.24	3.50E-07	1.19E-05
P31939	ATIC	14.98	23.64	3.75E-07	1.24E-05
Q14204	DYNC1H1	2.66	26.12	3.83E-07	1.24E-05
Q9GZU7-1	CTDSP1	-15.09	14.37	4.58E-07	1.44E-05
O94804	STK10	4.66	27.81	4.94E-07	1.53E-05
Q08722	CD47	11.32	18.71	5.49E-07	1.64E-05
P35580-2	MYH10	-3.12	26.85	5.54E-07	1.64E-05
Q96KN2	CNDP1	-1.81	25.67	7.04E-07	2.04E-05
P30086	PEBP1	3.27	25.98	1.04E-06	2.97E-05
P12883	MYH7	3.70	23.84	1.11E-06	3.09E-05
P28074-1	PSMB5	-3.69	24.34	1.17E-06	3.19E-05
Q9UDY2	TJP2	1.47	24.67	1.48E-06	3.96E-05
P14923	JUP	-2.06	27.46	1.55E-06	4.08E-05
P22891-1	PROZ	2.27	24.78	1.93E-06	4.98E-05
P01042-2	KNG1	-1.26	30.80	2.10E-06	5.32E-05
P07357	C8A	-1.79	28.60	2.33E-06	5.81E-05
P61981	YWHAG	-1.55	26.47	2.74E-06	6.71E-05
Q5JWF2-2	GNAS	2.54	23.46	2.93E-06	7.06E-05
Q05682-4	CALD1	3.21	28.82	3.81E-06	9.03E-05
P00491	PNP	2.71	26.52	4.10E-06	9.55E-05
P62258-1	YWHAE	2.20	28.28	4.22E-06	9.67E-05
P35241-5	RDX	-3.01	24.04	5.57E-06	1.26E-04
P62158	NA	1.28	27.19	5.96E-06	1.32E-04
P10619	CTSA	-2.12	23.39	6.30E-06	1.38E-04
O00712-4	NFIB	4.63	28.91	7.53E-06	1.62E-04
Q8WV44-1	TRIM41	8.76	19.42	1.25E-05	2.66E-04
Q9NZN3	EHD3	1.26	26.09	1.34E-05	2.79E-04
O60925	PFDN1	8.25	10.97	1.42E-05	2.91E-04
P00451	F8	-2.08	24.82	1.46E-05	2.94E-04
A0A0B4J1X5	NA	-3.50	25.20	1.47E-05	2.94E-04
P50991	CCT4	1.36	25.53	1.71E-05	3.38E-04
Q27J81-2	INF2	-2.36	24.75	1.82E-05	3.51E-04
P33121	ACSL1	11.43	19.57	1.83E-05	3.51E-04
P08758	ANXA5	2.40	24.03	1.87E-05	3.52E-04
P19652	ORM2	2.10	24.78	1.89E-05	3.52E-04
P29375-1	KDM5A	-1.83	26.02	2.48E-05	4.53E-04

Q6ZVX7	NCCRP1	2.40	24.08	2.49E-05	4.53E-04
Q08830	FGL1	2.65	25.92	2.55E-05	4.58E-04
Q6UWP8-1	SBSN	4.00	27.51	2.71E-05	4.81E-04
Q4KMQ2-3	ANO6	2.41	24.42	2.88E-05	5.05E-04
P49593	PPM1F	-9.98	20.46	3.02E-05	5.24E-04
P07988	SFTPB	-6.52	24.21	3.23E-05	5.53E-04
Q9UK55	SERPINA10	-1.35	26.28	3.35E-05	5.66E-04
P09871	C1S	-1.10	29.32	3.44E-05	5.76E-04
P08238	HSP90AB1	-1.56	25.66	4.81E-05	7.85E-04
P50851-1	LRBA	2.82	24.13	5.09E-05	8.23E-04
P0C0L4-1	C4A	1.22	28.53	5.29E-05	8.44E-04
P48059	LIMS1	-1.59	27.89	5.69E-05	8.98E-04
Q13740-2	ALCAM	10.32	14.29	5.94E-05	9.28E-04
Q08431	MFGE8	10.49	19.98	6.02E-05	9.29E-04
Q06187	BTK	-2.02	23.52	6.08E-05	9.29E-04
P06331	NA	1.81	28.08	6.33E-05	9.58E-04
P01717	NA	2.14	27.91	6.66E-05	9.96E-04
P02747	C1QC	2.06	29.44	6.73E-05	9.96E-04
P53990-5	IST1	-4.06	24.38	6.86E-05	9.97E-04
Q8NEY1-3	NAV1	2.15	29.52	6.88E-05	9.97E-04
Q01629	IFITM2	8.84	21.63	7.84E-05	1.13E-03
P40227-1	CCT6A	-1.18	24.99	7.96E-05	1.13E-03
P09110-1	ACAA1	13.82	15.58	8.05E-05	1.13E-03
P05771-2	PRKCB	-2.08	25.43	8.81E-05	1.22E-03
P48735	IDH2	-1.10	26.57	9.39E-05	1.28E-03
O75923-3	DYSF	2.30	26.14	9.51E-05	1.29E-03
P48444	ARCN1	-8.08	11.15	1.28E-04	1.72E-03
P29401	TKT	-1.44	24.76	1.30E-04	1.72E-03
O43396	TXNL1	3.55	23.88	1.41E-04	1.84E-03
Q96Q06-1	NA	-5.42	24.63	1.43E-04	1.85E-03
P05091	ALDH2	-8.50	11.88	1.48E-04	1.90E-03
Q8NF91-7	SYNE1	1.27	26.15	1.51E-04	1.92E-03
O15078-1	CEP290	1.42	29.97	1.62E-04	2.02E-03
Q99832	CCT7	1.44	25.48	1.62E-04	2.02E-03
O00410	IPO5	10.58	13.12	1.69E-04	2.08E-03
Q9NP72	RAB18	10.31	11.92	1.76E-04	2.16E-03
O75563	SKAP2	-2.01	24.79	1.90E-04	2.28E-03
Q9Y6E0	STK24	1.95	25.87	1.90E-04	2.28E-03
Q9P270	SLAIN2	-12.20	16.96	1.91E-04	2.28E-03
P01859	NA	2.14	27.28	2.25E-04	2.67E-03

P20701-1	ITGAL	-3.61	23.92	2.29E-04	2.69E-03
Q12805	EFEMP1	-1.91	29.10	2.40E-04	2.80E-03
P04792	HSPB1	1.18	24.54	2.75E-04	3.15E-03
P34897-1	SHMT2	-10.78	12.77	2.81E-04	3.19E-03
Q13045-2	FLII	-9.24	14.23	2.83E-04	3.19E-03
P49748-1	ACADVL	7.97	24.09	3.10E-04	3.47E-03
Q07065	CKAP4	11.44	13.65	3.26E-04	3.62E-03
Q5D862	FLG2	1.51	27.20	3.28E-04	3.62E-03
P02765	AHSG	-1.02	31.23	3.54E-04	3.87E-03
Q3V6T2-1	CCDC88A	-1.76	25.24	3.78E-04	4.10E-03
P04843	RPN1	-1.54	23.45	3.90E-04	4.19E-03
O60240	PLIN1	2.34	24.66	4.18E-04	4.47E-03
Q9H813-2	PACC1	-1.73	28.17	4.32E-04	4.58E-03
Q02108	GUCY1A1	-10.60	14.04	4.61E-04	4.81E-03
Q9NPQ8	RIC8A	7.12	10.84	4.71E-04	4.88E-03
P01591	JCHAIN	1.75	28.84	4.74E-04	4.88E-03
Q9H7C9-1	AAMDC	-11.08	15.99	5.13E-04	5.25E-03
P13224-2	GP1BB	1.50	27.62	5.19E-04	5.25E-03
Q15848	ADIPOQ	9.91	19.16	5.24E-04	0.005254601
P01137	TGFB1	1.19	25.65	5.25E-04	0.005254601
Q9UPN3	MACF1	1.79	26.42	5.30E-04	0.005261886
P30046	DDT	10.19	16.70	5.45E-04	0.005364479
Q14697-1	GANAB	-2.19	23.50	5.47E-04	0.005364479
P30043	BLVRB	-1.30	25.91	5.57E-04	0.005417944
O75342	ALOX12B	2.20	24.40	5.70E-04	0.005512421
P51606-1	RENBP	2.89	25.73	5.88E-04	0.00564696
Q14642	INPP5A	-10.54	18.52	6.05E-04	0.005764073
Q9C0C9	UBE2O	2.56	25.28	6.10E-04	0.005764073
Q9UKV8	AGO2	6.97	23.81	6.13E-04	0.005764073
P00915	CA1	-1.35	29.34	6.58E-04	0.006155682
P23229-6	ITGA6	-1.20	27.49	8.09E-04	0.007516714
P33176	KIF5B	-8.04	18.58	8.26E-04	0.007624559
Q9UI12-2	ATP6V1H	-9.50	18.97	8.66E-04	0.007942715
P00492	HPRT1	-5.05	22.83	8.85E-04	0.008061382
Q96A32	MYLPF	8.96	20.65	9.33E-04	0.008447205
Q9H2K8	TAOK3	1.29	25.13	9.51E-04	0.008460597
Q00796	SORD	6.24	10.62	9.52E-04	0.008460597
O00233-1	PSMD9	-2.42	22.59	9.53E-04	0.008460597
P12273	PIP	2.54	25.71	9.61E-04	0.008478476
P20645	M6PR	10.35	15.40	9.71E-04	0.008517565

P78559-1	MAP1A	-8.07	11.11	1.01E-03	0.008797634
Q03164	KMT2A	1.39	28.80	1.03E-03	0.008859404
P40763	STAT3	-2.65	21.71	1.05E-03	0.008964098
P20292	ALOX5AP	-13.16	15.39	1.10E-03	0.009262843
Q9NR12-1	PDLIM7	2.29	23.67	1.11E-03	0.009262843
Q8NI99	ANGPTL6	-1.70	24.70	1.12E-03	0.009262843
O75347	TBCA	-9.95	16.62	1.12E-03	0.009262843
O00161	SNAP23	-1.03	25.46	1.12E-03	0.009262843
P20042	EIF2S2	-8.74	14.77	1.13E-03	0.009262843
P07359	GP1BA	1.05	28.05	1.13E-03	0.009262843
Q7Z2W4	ZC3HAV1	9.30	19.51	1.16E-03	0.009513507
P45974-1	USP5	1.36	23.84	1.22E-03	0.009929971
P53396-2	ACLY	-1.67	26.33	1.26E-03	0.010146173
P10643	C7	1.06	28.43	1.29E-03	0.010307491
Q13094	LCP2	-1.71	23.52	1.43E-03	0.011189938
Q08495-1	DMTN	2.10	28.85	1.43E-03	0.011189938
Q96AC1	FERMT2	9.76	12.00	1.48E-03	0.011454704
Q68BL7-2	OLFML2A	7.79	17.81	1.57E-03	0.012087113
Q9Y251	HPSE	7.44	22.29	1.62E-03	0.012385661
P08253-3	MMP2	-1.68	23.96	1.67E-03	0.01270924
Q8TCU4-1	ALMS1	-11.61	13.96	1.74E-03	0.013175427
O75791	GRAP2	3.02	22.79	1.75E-03	0.01318756
P02743	APCS	-1.16	27.14	1.76E-03	0.01318756
P04233-1	CD74	10.86	17.25	1.79E-03	0.013344837
Q86UD1	OAF	7.29	20.34	1.98E-03	0.014657204
P37840-1	SNCA	-1.37	27.02	2.04E-03	0.015049262
Q8NEU8-1	APPL2	-10.65	15.09	2.08E-03	0.015256901
Q99972	MYOC	-9.50	17.73	2.13E-03	0.015545238
P78509	RELN	1.26	25.36	2.44E-03	0.017440125
Q9UBV8	PEF1	-9.95	12.76	2.44E-03	0.017440125
Q05209-1	PTPN12	1.47	24.64	2.45E-03	0.017440125
P11234-2	RALB	1.57	25.44	2.46E-03	0.017440125
P31146	CORO1A	-1.03	26.92	2.47E-03	0.017440125
P07384	CAPN1	-1.22	26.29	2.56E-03	0.017907687
Q15722	LTB4R	7.91	22.19	2.57E-03	0.017907687
Q96QA5	GSDMA	-1.46	24.13	2.66E-03	0.018461905
Q9Y4F9	RIPOR2	-5.70	22.11	2.81E-03	0.019266274
P05161	ISG15	-11.00	14.23	2.83E-03	0.019334685
Q7LDG7-2	RASGRP2	-1.68	25.21	3.20E-03	0.0216484
Q96P48-6	ARAP1	-9.78	14.09	3.36E-03	0.02234964

Q6ZQQ6-1	WDR87	-2.39	25.87	3.36E-03	0.02234964
P29966	MARCKS	-2.08	24.89	3.37E-03	0.02234964
Q8N4C8-3	MINK1	3.28	21.64	3.38E-03	0.02234964
P18054	ALOX12	1.89	23.98	3.46E-03	0.022782122
P14314-2	PRKCSH	-1.67	23.64	3.50E-03	0.022935577
Q7Z4W1	DCXR	3.22	22.39	3.66E-03	0.023878103
Q9UN19-1	DAPP1	-10.16	14.27	0.003906652	0.025233421
P25685	DNAJB1	4.52	23.47	0.004140287	0.026621483
Q4KMP7	TBC1D10B	1.49	24.22	0.004269819	0.027330691
P50502	ST13	-1.15	25.05	0.004428549	0.028219586
P02746	C1QB	1.60	29.08	0.004528046	0.028597126
P15311	EZR	-1.69	23.85	0.004595332	0.028766372
Q14525	KRT33B	-6.39	19.91	0.004744152	0.029567717
Q9HDC9	APMAP	-1.16	28.56	0.004797128	0.029767328
P02745	C1QA	2.13	27.92	0.004856674	0.029842267
P46940	IQGAP1	1.04	26.25	0.004861863	0.029842267
P01721	NA	6.85	12.54	0.004872207	0.029842267
P00739-1	HPR	1.07	27.83	0.005049689	0.0307966
P62491-1	RAB11A	1.17	26.68	0.005079652	0.030846947
Q9Y3I1-2	FBXO7	9.97	17.89	0.005117275	0.030893598
P51809	VAMP7	5.89	11.25	0.005145596	0.030893598
P81605	DCD	-1.16	28.43	0.005237253	0.03126948
O15144	ARPC2	1.06	27.78	0.005619646	0.033272987
P43490	NAMPT	-7.94	14.54	0.005700188	0.03360982
Q9H2G2-2	SLK	6.32	24.24	0.006000385	0.035233667
P30626-1	SRI	1.28	24.46	0.00611627	0.035766338
P16070-7	CD44	-1.34	23.83	0.006580333	0.038010784
P63104-1	YWHAZ	-1.25	28.66	0.007443555	0.042185261
P00367	GLUD1	-8.32	15.34	0.007456405	0.042185261
P10124	SRGN	2.27	22.68	0.007458075	0.042185261
Q9HC84	MUC5B	-9.01	16.50	0.007666853	0.043061655
P07900-2	HSP90AA1	-1.41	27.82	0.007797469	0.04362285
Q01995	TAGLN	5.97	20.88	0.008011462	0.044307471
Q8N699	MYCT1	-4.64	22.57	0.00803499	0.044307471
A0A075B6J9	NA	1.71	23.89	0.008044566	0.044307471
O43639	NCK2	-1.42	23.46	0.008391862	0.046041839
P20700	LMNB1	-6.78	13.19	0.008669338	0.047381267
Q9Y376	CAB39	-1.43	24.26	0.008732565	0.047543965
O76074	PDE5A	1.35	28.69	0.009066476	0.049173521
P11233	RALA	-1.53	24.23	0.009133672	0.049349611

Table 4: Appendix 3. Differential EV protein expression due to the T2DM-by-COVID-19 interaction effect.

Uniprot	SYMBOL	logFC	AveExpr	P.Value	adj.P.Val
P09543-1	CNP	-5.11	25.85	6.75E-19	9.60E-16
O60281-1	ZNF292	6.36	26.27	7.45E-18	5.29E-15
Q96CX2	KCTD12	5.05	26.55	1.31E-16	6.21E-14
P15291-2	B4GALT1	3.58	24.95	2.86E-15	1.02E-12
P42680	TEC	16.05	14.23	1.27E-14	3.61E-12
P0C0L4-1	C4A	-2.83	28.53	9.50E-14	2.25E-11
Q14247-1	CTTN	3.28	27.42	3.41E-13	6.92E-11
Q9NVA2-1	SEPTIN11	4.21	25.21	6.05E-13	1.07E-10
Q13287	NMI	19.40	14.31	6.90E-13	1.09E-10
Q13642	FHL1	4.80	27.84	1.21E-12	1.72E-10
O15400-2	STX7	-4.14	26.22	1.94E-12	2.51E-10
Q9NYC9-1	DNAH9	-2.03	27.91	2.84E-12	3.36E-10
Q99685-1	MGLL	-19.93	18.19	6.42E-12	7.02E-10
P14770	GP9	2.24	27.57	8.96E-12	9.10E-10
Q14203-3	DCTN1	-3.60	25.42	1.43E-10	1.34E-08
P22061	PCMT1	4.63	25.23	1.51E-10	1.34E-08
P02814	SMR3B	-11.26	19.61	2.81E-10	2.35E-08
Q13740-2	ALCAM	17.66	14.29	6.68E-10	5.27E-08
Q68EM7	ARHGAP17	20.31	16.18	8.70E-10	6.45E-08
Q9UIB8	CD84	-3.20	24.99	9.08E-10	6.45E-08
A0A0B4J1X5	NA	5.33	25.20	1.19E-09	7.81E-08
O43294-1	TGFB1I1	2.84	24.42	1.21E-09	7.81E-08
Q13201	MMRN1	1.54	28.51	1.98E-09	1.22E-07
Q5TDH0-3	DDI2	3.85	26.86	2.40E-09	1.42E-07
O15117-3	FYB1	2.65	26.42	3.58E-09	2.04E-07
Q99972	MYOC	20.51	17.73	4.71E-09	2.58E-07
Q6BDS2	UHRF1BP1	-19.20	20.29	5.44E-09	2.86E-07
P37837	TALDO1	-2.21	25.05	5.96E-09	3.02E-07
P30086	PEBP1	-3.97	25.98	7.21E-09	3.53E-07
P05141	SLC25A5	-1.91	26.26	7.55E-09	3.57E-07
P48426	PIP4K2A	9.84	11.37	1.24E-08	5.69E-07
P62158	NA	-1.66	27.19	1.40E-08	6.24E-07
Q08722	CD47	-12.85	18.71	1.54E-08	6.65E-07
P52209	PGD	-5.63	29.28	1.84E-08	7.71E-07
P06681-1	C2	2.02	27.17	2.19E-08	8.90E-07
Q7L7X3	TAOK1	5.24	22.00	4.00E-08	1.58E-06
P26572	MGAT1	3.33	26.39	4.45E-08	1.71E-06

Q5SW79-1	CEP170	-3.07	24.79	5.57E-08	2.08E-06
P49908	SELENOP	-1.73	28.37	7.86E-08	2.86E-06
P62258-1	YWHAE	-2.56	28.28	1.05E-07	3.72E-06
P31939	ATIC	-15.22	23.64	1.14E-07	3.97E-06
P01011-1	SERPINA3	-2.17	30.13	1.38E-07	4.67E-06
Q9UPN3	MACF1	-2.89	26.42	1.45E-07	4.78E-06
Q27J81-2	INF2	2.90	24.75	2.18E-07	7.06E-06
Q9H299	SH3BGRL3	4.38	24.77	2.43E-07	7.66E-06
P0DOX2	NA	-1.87	29.31	2.75E-07	8.49E-06
Q05682-4	CALD1	-3.47	28.82	4.11E-07	1.24E-05
Q9GZU7-1	CTDSP1	14.51	14.37	4.28E-07	1.27E-05
Q5JWF2-2	GNAS	-2.68	23.46	4.86E-07	1.41E-05
P08571	CD14	-2.07	27.47	5.47E-07	1.55E-05
P61769	B2M	-2.00	26.26	5.57E-07	1.55E-05
P50991	CCT4	-1.59	25.53	5.80E-07	1.59E-05
P37840-1	SNCA	-2.31	27.02	7.90E-07	2.12E-05
O75923-3	DYSF	-2.95	26.14	8.53E-07	2.25E-05
Q13045-2	FLII	12.81	14.23	9.89E-07	2.53E-05
P07988	SFTPB	7.68	24.21	9.97E-07	2.53E-05
P23467	PTPRB	9.56	23.37	1.06E-06	2.64E-05
Q9UDY2	TJP2	-1.43	24.67	1.08E-06	2.64E-05
P33121	ACSL1	-12.90	19.57	1.11E-06	2.68E-05
Q6ZVX7	NCCRP1	-2.75	24.08	1.16E-06	2.73E-05
P29350-3	PTPN6	-2.02	25.90	1.18E-06	2.73E-05
P22303-1	ACHE	-3.04	25.79	1.19E-06	2.73E-05
Q14766-4	LTBP1	-1.12	28.47	1.33E-06	3.00E-05
Q96Q06-1	NA	6.98	24.63	1.43E-06	3.18E-05
P10809	HSPD1	-3.69	26.31	2.38E-06	5.18E-05
Q5D862	FLG2	-2.02	27.20	2.42E-06	5.18E-05
P08754	GNAI3	-1.18	25.03	2.44E-06	5.18E-05
Q14204	DYNC1H1	-2.31	26.12	2.51E-06	5.24E-05
O15144	ARPC2	-1.89	27.78	2.67E-06	5.51E-05
O95236-1	APOL3	14.77	18.01	3.72E-06	7.56E-05
P30626-1	SRI	-2.24	24.46	4.28E-06	8.56E-05
O00712-4	NFIB	-4.57	28.91	4.50E-06	8.87E-05
Q03164	KMT2A	-1.99	28.80	4.87E-06	9.48E-05
Q99832	CCT7	-1.74	25.48	4.95E-06	9.49E-05
P40926	MDH2	-1.75	25.49	5.01E-06	9.49E-05
Q9NR12-1	PDLIM7	3.28	23.67	5.29E-06	9.89E-05
P04080	CSTB	1.41	24.32	6.05E-06	1.12E-04

Q9NQC3	RTN4	1.78	24.52	6.84E-06	1.25E-04
P00491	PNP	-2.49	26.52	7.90E-06	1.42E-04
O60240	PLIN1	-2.94	24.66	1.04E-05	1.84E-04
Q13464	ROCK1	13.31	14.58	1.10E-05	1.92E-04
P48059	LIMS1	1.68	27.89	1.43E-05	2.45E-04
P05771-2	PRKCB	2.24	25.43	1.62E-05	2.74E-04
Q9Y2A7-1	NCKAP1	-1.63	23.41	1.87E-05	3.13E-04
Q9HDC9	APMAP	1.79	28.56	1.96E-05	3.23E-04
Q08495-1	DMTN	-2.82	28.85	2.16E-05	3.53E-04
Q01546	KRT76	8.70	23.89	2.24E-05	3.61E-04
P23229-6	ITGA6	1.50	27.49	2.74E-05	4.37E-04
Q8NEY1-3	NAV1	-2.19	29.52	2.79E-05	4.40E-04
P51665	PSMD7	-11.33	12.65	2.84E-05	4.43E-04
P20701-1	ITGAL	4.02	23.92	2.93E-05	4.48E-04
Q9C075	KRT23	2.22	23.55	2.93E-05	4.48E-04
Q9NYL9	TMOD3	-2.05	24.91	3.01E-05	4.50E-04
P48509	CD151	-12.95	19.02	3.01E-05	4.50E-04
Q4KMP7	TBC1D10B	-2.21	24.22	3.11E-05	4.60E-04
P07357	C8A	1.46	28.60	3.24E-05	4.74E-04
P32320	CDA	-10.56	18.82	3.27E-05	4.74E-04
Q14344	GNA13	5.55	23.21	3.48E-05	5.00E-04
Q07960	ARHGAP1	2.82	25.24	3.65E-05	5.19E-04
Q99623	PHB2	6.15	23.95	3.84E-05	5.40E-04
P08238	HSP90AB1	1.50	25.66	4.81E-05	6.70E-04
Q68BL7-2	OLFML2A	-9.98	17.81	5.05E-05	6.94E-04
O15056	SYNJ2	1.89	27.07	5.08E-05	6.94E-04
P02765	AHSG	1.13	31.23	5.34E-05	7.22E-04
P00451	F8	1.82	24.82	5.66E-05	7.59E-04
P68036	UBE2L3	-12.36	15.50	5.90E-05	7.83E-04
P19634-1	SLC9A1	14.19	16.45	6.76E-05	8.82E-04
P19013	NA	1.38	28.77	6.90E-05	8.91E-04
P49748-1	ACADVL	-8.56	24.09	7.24E-05	9.27E-04
Q8WV44-1	TRIM41	-7.46	19.42	7.35E-05	9.32E-04
Q9BUL8	PDCD10	1.13	24.44	7.74E-05	9.71E-04
Q9UKV8	AGO2	-7.91	23.81	7.79E-05	9.71E-04
P01717	NA	-2.02	27.91	8.14E-05	1.01E-03
P48444	ARCN1	7.98	11.15	8.61E-05	1.05E-03
Q9NQ79	CRTAC1	-1.85	24.08	9.21E-05	1.12E-03
Q02108	GUCY1A1	11.56	14.04	9.30E-05	1.12E-03
Q9H939-1	PSTPIP2	4.68	26.77	9.74E-05	1.16E-03

P15311	EZR	2.33	23.85	1.04E-04	1.23E-03
P05062	ALDOB	-1.60	25.38	1.09E-04	1.28E-03
P20042	EIF2S2	10.12	14.77	1.27E-04	1.48E-03
P27701	CD82	9.72	20.61	1.41E-04	1.63E-03
P50995	ANXA11	1.75	25.39	1.44E-04	1.65E-03
Q16775-2	HAGH	-2.35	25.28	1.49E-04	1.70E-03
Q00796	SORD	7.00	10.62	1.55E-04	1.75E-03
P02743	APCS	1.38	27.14	1.61E-04	1.80E-03
Q99549	MPHOSPH8	-1.75	26.73	1.63E-04	1.81E-03
P33151	CDH5	2.13	25.53	1.72E-04	1.89E-03
P29144	TPP2	-2.61	25.46	1.85E-04	2.01E-03
P00387-2	CYB5R3	2.20	24.88	1.93E-04	2.08E-03
P27918	CFP	11.03	20.20	2.02E-04	2.15E-03
P14923	JUP	1.44	27.46	2.04E-04	2.15E-03
P05091	ALDH2	7.94	11.88	2.05E-04	2.15E-03
P16152	CBR1	-7.91	23.50	2.06E-04	2.15E-03
P27348	YWHAQ	-2.34	27.51	2.07E-04	2.15E-03
O14745	SLC9A3R1	1.98	25.28	2.12E-04	2.18E-03
Q9H2G2-2	SLK	-8.48	24.24	2.16E-04	0.0022051
P42574	CASP3	-6.95	25.44	2.40E-04	0.002431367
Q08188	TGM3	-1.98	26.64	2.55E-04	0.002571116
O60763-2	USO1	-12.27	20.81	2.69E-04	0.002687365
P62491-1	RAB11A	-1.51	26.68	2.79E-04	0.002772981
P01859	NA	-2.00	27.28	3.03E-04	0.002987141
P80108	GPLD1	-1.15	26.73	3.07E-04	0.003011981
Q14677-3	CLINT1	3.35	24.28	3.11E-04	0.003028396
Q9NRY5	FAM114A2	5.64	11.71	3.21E-04	0.003085775
Q8NEU8-1	APPL2	12.20	15.09	3.21E-04	0.003085775
P23526-1	AHCY	1.05	24.38	3.33E-04	0.003178763
Q01629	IFITM2	-7.56	21.63	3.38E-04	0.003201093
P12883	MYH7	-2.41	23.84	3.71E-04	0.003495426
Q9H0B8	CRISPLD2	-5.11	10.18	3.79E-04	0.003544234
Q92973-1	TNPO1	-12.41	20.64	3.88E-04	0.003580885
O60925	PFDN1	6.20	10.97	3.88E-04	0.003580885
O43707	ACTN4	1.68	26.07	3.96E-04	0.003631026
Q86YW5-2	TREML1	-1.44	23.86	4.00E-04	0.003639797
Q9Y251	HPSE	-8.08	22.29	4.39E-04	0.003944885
Q96P48-6	ARAP1	11.48	14.09	4.51E-04	0.004031058
Q15848	ADIPOQ	9.59	19.16	4.70E-04	0.004178509
P04792	HSPB1	-1.07	24.54	4.93E-04	0.004355404

P23528	CFL1	1.05	29.17	5.60E-04	0.00488089
P51606-1	RENBP	-2.77	25.73	5.73E-04	0.004952675
P43034	PAFAH1B1	-9.02	26.20	5.75E-04	0.004952675
Q13404	UBE2V1	8.86	17.41	5.84E-04	0.004999947
P19320-3	VCAM1	-2.77	24.62	6.40E-04	0.005443571
Q6UWP8-1	SBSN	-2.98	27.51	6.82E-04	0.005764653
O00231	PSMD11	11.21	18.67	7.02E-04	0.005906638
P53396-2	ACLY	1.69	26.33	7.09E-04	0.005923065
P28074-1	PSMB5	2.27	24.34	7.19E-04	0.00596255
P09493-8	TPM1	-1.05	25.94	7.22E-04	0.00596255
O75342	ALOX12B	-2.04	24.40	7.99E-04	0.006559812
P63104-1	YWHAZ	1.54	28.66	8.04E-04	0.006567493
P61006	RAB8A	-1.23	24.26	8.22E-04	0.006661275
P06729	CD2	7.65	17.13	8.25E-04	0.006661275
O75015	FCGR3B	3.00	23.50	8.59E-04	0.0068577
Q9NRW1	RAB6B	-2.34	24.98	9.55E-04	0.007539169
P01817	NA	-4.75	22.65	9.62E-04	0.007550392
P07359	GP1BA	-1.03	28.05	9.67E-04	0.007550392
Q14974	KPNB1	-1.26	23.22	9.82E-04	0.007628464
Q8N4C8-3	MINK1	-3.58	21.64	1.01E-03	0.00777828
P31146	CORO1A	1.08	26.92	1.04E-03	0.007954731
Q86TH1	ADAMTSL2	-1.75	25.69	1.06E-03	0.008058183
Q03001-8	DST	-1.27	27.81	1.11E-03	0.008337143
Q92619	ARHGAP45	3.28	21.50	1.16E-03	0.008674425
P21281	ATP6V1B2	3.06	23.63	1.17E-03	0.008697656
P01137	TGFB1	-1.05	25.65	1.22E-03	0.009056305
P28062-1	PSMB8	-10.85	16.25	1.24E-03	0.009097972
Q8NI99	ANGPTL6	1.61	24.70	1.25E-03	0.009127232
P0DJI8	SAA1	-2.21	29.45	1.26E-03	0.009166031
Q4KMQ2-3	ANO6	-1.70	24.42	1.27E-03	0.009166031
P17987	TCP1	-1.60	23.95	1.31E-03	0.009370756
Q86VP6-1	CAND1	1.42	22.93	1.31E-03	0.009370756
Q9H2K8	TAOK3	-1.20	25.13	1.33E-03	0.009440734
P61020	RAB5B	1.80	25.18	1.35E-03	0.00957916
O94804	STK10	-2.57	27.81	1.42E-03	0.009959385
P20340-1	RAB6A	-2.07	24.07	1.46E-03	0.010237788
Q9H479	FN3K	-4.37	23.97	1.50E-03	0.010480961
Q13200	PSMD2	-1.40	25.10	1.56E-03	0.010839359
P04279-1	SEMG1	8.24	16.34	1.62E-03	0.011131141
P11766	ADH5	8.64	17.47	1.76E-03	0.011950754

P07858	CTSB	9.33	17.38	1.80E-03	0.012196276
P53814-1	SMTN	7.70	15.70	1.98E-03	0.013205413
Q10567	AP1B1	-8.68	17.01	1.98E-03	0.013205413
Q15722	LTB4R	-7.80	22.19	1.98E-03	0.013205413
O95466-3	FMNL1	4.65	23.55	2.04E-03	0.013525276
P11836	MS4A1	-8.37	19.98	2.08E-03	0.013678596
P02533	KRT14	1.23	30.51	0.002132472	0.013900196
Q15323	KRT31	-9.76	19.85	0.002254654	0.014629516
P09525	ANXA4	9.46	13.14	0.00229067	0.014795647
Q9H4F8-2	SMOC1	-9.21	16.40	0.002406854	0.015336946
Q9BX67	JAM3	1.42	24.08	0.002436725	0.01539512
P07947	YES1	7.72	20.01	0.002437651	0.01539512
Q9BT78	COPS4	-8.16	12.43	0.0025107	0.015786306
P05452	CLEC3B	1.10	25.63	0.00255136	0.015971288
Q16891	IMMT	-6.55	12.86	0.002730996	0.017020811
P11279	LAMP1	8.39	15.75	0.002787261	0.017295626
P13667	PDIA4	1.78	24.23	0.002842332	0.017484649
P51809	VAMP7	-5.99	11.25	0.003153249	0.019169025
P12273	PIP	-2.12	25.71	0.003505917	0.021020711
Q9H444	CHMP4B	-1.19	26.10	0.003525667	0.021050306
P14209	CD99	-3.91	24.26	0.003590138	0.021345551
Q9UGM5-1	FETUB	-2.08	27.34	0.003613571	0.021395352
P02649	APOE	-1.03	32.73	0.003779533	0.022193044
Q8NF50-1	DOCK8	-4.98	22.69	0.003826714	0.022377617
P04234	CD3D	-7.76	19.04	0.004031219	0.023476893
O00186	STXBP3	9.29	16.09	0.004083249	0.023626894
P06703	S100A6	1.66	25.20	0.004090229	0.023626894
Q8N392-1	ARHGAP18	1.02	25.16	0.004112997	0.02366222
P06730	EIF4E	-6.88	13.23	0.004255387	0.024100144
O75791	GRAP2	-2.61	22.79	0.004255714	0.024100144
P15170-3	GSPT1	8.70	15.09	0.004256957	0.024100144
P06127	CD5	-8.23	14.96	0.004594171	0.02590602
O43396	TXNL1	-2.43	23.88	0.004636225	0.026039825
Q9UBV8	PEF1	8.83	12.76	0.004692558	0.026207855
P08648	ITGA5	-1.04	23.09	0.004703028	0.026207855
P16070-7	CD44	1.34	23.83	0.004828221	0.02678242
P05161	ISG15	9.89	14.23	0.00484383	0.02678242
P54727	RAD23B	-9.16	13.63	0.004968408	0.027364761
P55259-1	GP2	-8.20	14.42	0.005042203	0.027591447
P06312	NA	1.83	26.37	0.0050484	0.027591447

Q9UKE5-4	TNIK	-8.28	19.93	0.005068524	0.027595297
Q14315	FLNC	8.72	18.05	0.005119436	0.027660526
P21980	TGM2	-1.88	23.23	0.005203885	0.028010303
P01019	AGT	-1.29	25.43	0.005504349	0.029515776
A0A0B4J1V0	NA	1.39	26.86	0.005666686	0.030162269
P48061	CXCL12	9.16	15.27	0.005667365	0.030162269
Q15149-7	PLEC	-1.36	28.23	0.005809855	0.030796762
P30046	DDT	-7.57	16.70	0.005829929	0.030796762
Q9BQ50-1	TREX2	8.63	13.31	0.005868665	0.030886564
Q9Y696	CLIC4	1.03	25.37	0.005965929	0.031179395
P62942	FKBP1A	1.62	24.00	0.00599013	0.031179395
P41250	GARS1	-5.33	22.07	0.006038298	0.031205627
O14672	ADAM10	1.05	24.71	0.00603909	0.031205627
P50990	CCT8	-1.15	25.62	0.006149841	0.031662767
P22891-1	PROZ	1.13	24.78	0.006336201	0.032504481
P11234-2	RALB	1.34	25.44	0.006409058	0.032759967
P46976-1	GYG1	5.89	20.12	0.006477689	0.032992102
P16671	CD36	1.66	25.54	0.006608396	0.033537611
P07384	CAPN1	1.04	26.29	0.00688259	0.034681418
P23083	NA	-1.30	27.99	0.006977825	0.035037063
P52943	CRIP2	-7.11	17.75	0.007067049	0.035360127
P55287-1	CDH11	-4.00	24.67	0.007320496	0.036245381
P01591	JCHAIN	-1.24	28.84	0.007408853	0.036555489
Q03154-1	ACY1	-7.79	17.24	0.007603251	0.037254148
P12035	KRT3	8.58	18.89	0.007629104	0.037254148
Q9UHD9	UBQLN2	-9.15	14.86	0.007945677	0.038443951
Q9BS26	ERP44	-3.77	23.64	0.007953921	0.038443951
Q7Z4W1	DCXR	-2.79	22.39	0.008203648	0.039516558
P20963-1	CD247	8.49	15.96	0.008496667	0.040789742
P25685	DNAJB1	3.94	23.47	0.008556533	0.040938831
P61081	UBE2M	7.80	17.53	0.0086488	0.041239533
Q14697-1	GANAB	-1.54	23.50	0.008682584	0.041239533
O75832	PSMD10	5.32	11.50	0.008727546	0.041239533
P30405	PPIF	-5.56	11.53	0.008825594	0.041458599
Q5JSH3	WDR44	-1.39	24.84	0.008840222	0.041458599
P07900-2	HSP90AA1	1.32	27.82	0.008991619	0.042029903
P40939	HADHA	-5.74	13.93	0.009078883	0.042160434
P19367-1	HK1	-1.69	24.65	0.009154587	0.042373512
P15374	UCHL3	6.90	15.25	0.009391093	0.043327086
Q9UL46	PSME2	1.90	23.60	0.009708245	0.044216077

O14974-5	PPP1R12A	-1.90	24.03	0.009800917	0.044495536
P35611-3	ADD1	-2.35	24.68	0.009918218	0.044884675
P01033	TIMP1	1.28	22.46	0.01019178	0.045976251
Q6ZQQ6-1	WDR87	1.98	25.87	0.010401641	0.046774468
O15145	ARPC3	2.37	25.12	0.010576183	0.046977307
P62851	RPS25	6.74	15.63	0.010578985	0.046977307
Q9UEY8-1	ADD3	8.44	14.18	0.010649737	0.047054976
P23634-1	ATP2B4	-4.01	20.99	0.010662704	0.047054976
P55957-1	BID	-5.44	18.11	0.010759699	0.047326313
P35813	PPM1A	-5.56	20.93	0.010823728	0.047326313
P31947-1	SFN	-1.08	26.11	0.010860539	0.047326313
Q99808	SLC29A1	-7.03	18.50	0.010866958	0.047326313
P22352	GPX3	-1.56	27.09	0.010893308	0.047326313
Q3ZCW2	LGALSL	-1.22	23.85	0.010924019	0.047326313
P37802	TAGLN2	1.31	28.09	0.011359611	0.04906385
Q9Y266	NUDC	7.60	14.91	0.01143125	0.049192511
Q99733	NAP1L4	-5.98	20.02	0.011458636	0.049192511
P13804-1	ETFA	7.35	13.10	0.011533734	0.049365772
P51572-2	BCAP31	-1.48	23.33	0.011645454	0.049694264
Q9NVJ2	ARL8B	-7.46	16.38	0.011706354	0.049714735
P43686-2	PSMC4	4.21	21.09	0.011720223	0.049714735

References

Altan-Bonnet N. (2016). Extracellular vesicles are the Trojan horses of viral infection. Current opinion in microbiology, 32, 77–81. https://doi.org/10.1016/j.mib.2016.05.004

Apicella, M., Campopiano, M. C., Mantuano, M., Mazoni, L., Coppelli, A., & Del Prato, S. (2020). COVID-19 in people with diabetes: understanding the reasons for worse outcomes. The lancet. Diabetes & endocrinology, 8(9), 782–792. https://doi.org/10.1016/S2213-8587(20)30238-2

Aronson J. K. (2005). Biomarkers and surrogate endpoints. British journal of clinical pharmacology, 59(5), 491–494. https://doi.org/10.1111/j.1365-2125.2005.02435.x

Ayres J. S. (2020). A metabolic handbook for the COVID-19 pandemic. Nature metabolism, 2(7), 572–585. https://doi.org/10.1038/s42255-020-0237-2

Badierah, R. A., Uversky, V. N., & Redwan, E. M. (2021). Dancing with Trojan horses: an interplay between the extracellular vesicles and viruses. Journal of biomolecular structure & dynamics, 39(8), 3034–3060. https://doi.org/10.1080/07391102.2020.1756409

Barile, L., & Vassalli, G. (2017). Exosomes: Therapy delivery tools and biomarkers of diseases. Pharmacology & therapeutics, 174, 63–78. https://doi.org/10.1016/j.pharmthera.2017.02.020

Barron, E., Bakhai, C., Kar, P., Weaver, A., Bradley, D., Ismail, H., Knighton, P., Holman, N., Khunti, K., Sattar, N., Wareham, N. J., Young, B., & Valabhji, J. (2020). Associations of type 1 and type 2 diabetes with COVID-19-related mortality in England: a whole-population study. The lancet. Diabetes & endocrinology, 8(10), 813–822. https://doi.org/10.1016/S2213-8587(20)30272-2

Cañadas-Garre, M., Anderson, K., McGoldrick, J., Maxwell, A. P., & McKnight, A. J. (2019). Proteomic and metabolomic approaches in the search for biomarkers in chronic kidney disease. Journal of proteomics, 193, 93–122. https://doi.org/10.1016/j.jprot.2018.09.020

Ceriello, A. Coagulation activation in diabetes mellitus: the role of hyperglycaemia and therapeutic prospects. Diabetologia 36, 1119–1125 (1993). https://doi.org/10.1007/BF00401055

Ceriello A. (2020). Hyperglycemia and the worse prognosis of COVID-19. Why a fast blood glucose control should be mandatory. Diabetes research and clinical practice, 163, 108186. https://doi.org/10.1016/j.diabres.2020.108186

Ceriello, A., De Nigris, V., & Prattichizzo, F. (2020). Why is hyperglycaemia worsening COVID-19 and its prognosis?. Diabetes, obesity & metabolism, 22(10), 1951–1952. https://doi.org/10.1111/dom.14098

Elrashdy, F., Aljaddawi, A. A., Redwan, E. M., & Uversky, V. N. (2021). On the potential role of exosomes in the COVID-19 reinfection/reactivation opportunity. Journal of biomolecular structure & dynamics, 39(15), 5831–5842. https://doi.org/10.1080/07391102.2020.1790426

Erener S. (2020). Diabetes, infection risk and COVID-19. Molecular metabolism, 39, 101044. https://doi.org/10.1016/j.molmet.2020.101044

Feng, Z., Hensley, L., McKnight, K. L., Hu, F., Madden, V., Ping, L., Jeong, S. H., Walker, C., Lanford, R. E., & Lemon, S. M. (2013). A pathogenic picornavirus acquires an envelope by hijacking cellular membranes. Nature, 496(7445), 367–371. https://doi.org/10.1038/nature12029

Gould, S. J., Booth, A. M., & Hildreth, J. E. (2003). The Trojan exosome hypothesis. Proceedings of the National Academy of Sciences of the United States of America, 100(19), 10592–10597. https://doi.org/10.1073/pnas.1831413100

Hessvik, N. P., & Llorente, A. (2018). Current knowledge on exosome biogenesis and release. Cellular and molecular life sciences : CMLS, 75(2), 193–208. https://doi.org/10.1007/s00018-017-2595-9

Manne, B. K., Denorme, F., Middleton, E. A., Portier, I., Rowley, J. W., Stubben, C., Petrey, A. C., Tolley, N. D., Guo, L., Cody, M., Weyrich, A. S., Yost, C. C., Rondina, M. T., & Campbell, R. A. (2020). Platelet gene expression and function in patients with COVID-19. Blood, 136(11), 1317–1329. https://doi.org/10.1182/blood.2020007214

Margolis, L., & Sadovsky, Y. (2019). The biology of extracellular vesicles: The known unknowns. PLoS biology, 17(7), e3000363. https://doi.org/10.1371/journal.pbio.3000363

Mouri MI, Badireddy M. Hyperglycemia. [Updated 2021 May 10]. In: StatPearls [Internet]. Treasure Island (FL): StatPearls Publishing; 2022 Jan-. Available from: https://www.ncbi.nlm.nih.gov/books/NBK430900/

Powers, A. C., Aronoff, D. M., & Eckel, R. H. (2021). COVID-19 vaccine prioritisation for type 1 and type 2 diabetes. The lancet. Diabetes & endocrinology, 9(3), 140–141. https://doi.org/10.1016/S2213-8587(21)00017-6

Rajpal, A., Rahimi, L., & Ismail-Beigi, F. (2020). Factors leading to high morbidity and mortality of covid -19 in patients with type 2 diabetes. Journal of Diabetes, 12(12), 895–908. https://doi.org/10.1111/1753-0407.13085

Santiana, M., Ghosh, S., Ho, B. A., Rajasekaran, V., Du, W. L., Mutsafi, Y., De Jésus-Diaz, D. A., Sosnovtsev, S. V., Levenson, E. A., Parra, G. I., Takvorian, P. M., Cali, A., Bleck, C., Vlasova, A. N., Saif, L. J., Patton, J. T., Lopalco, P., Corcelli, A., Green, K. Y., & Altan-Bonnet, N. (2018). Vesicle-Cloaked Virus Clusters Are Optimal Units for Inter-organismal Viral Transmission. Cell host & microbe, 24(2), 208–220.e8. https://doi.org/10.1016/j.chom.2018.07.006

Shen, B., Yi, X., Sun, Y., Bi, X., Du, J., Zhang, C., Quan, S., Zhang, F., Sun, R., Qian, L., Ge, W., Liu, W., Liang, S., Chen, H., Zhang, Y., Li, J., Xu, J., He, Z., Chen, B., Wang, J., … Guo, T. (2020). Proteomic and Metabolomic Characterization of COVID-19 Patient Sera. Cell, 182(1), 59–72.e15. https://doi.org/10.1016/j.cell.2020.05.03

Nunez Lopez, Y.O., Iliuk, A., Petrilli, A., Glass, C., Casu, A., & Pratley, R. (2021). Defining the Proteomic and Phosphoproteomic Landscape of Circulating Extracellular Vesicles in the Diabetes Spectrum. MedRxIV. https://doi.org/10.1101/2021.10.31.21265724